Systematic Entomology

Systematic Entomology (2016), **41**, 541–566 DOI: 10.1111/syen.12173

Emergence of a superradiation: pselaphine rove beetles in mid-Cretaceous amber from Myanmar and their evolutionary implications

JOSEPH PARKER[1,2]

[1]Department of Genetics and Development, Columbia University, New York, NY, U.S.A. and [2]Division of Invertebrate Zoology, American Museum of Natural History, New York, NY, U.S.A.

Abstract. Pselaphinae is an exceptionally species-rich, globally distributed subfamily of minute rove beetles (Staphylinidae), many of which are inquilines of social insects. Deducing the factors that drove pselaphine diversification and their evolutionary predisposition to inquilinism requires a reliable timescale of pselaphine cladogenesis. Pselaphinae is split into a small and highly plesiomorphic supertribe, Faronitae, and its sister group, the 'higher Pselaphinae' – a vast multi-tribe clade with a more derived morphological ground plan, and which includes all known instances of inquilinism. The higher Pselaphinae is dominated by tribes with a Gondwanan taxonomic bias. However, a minority of tribes are limited to the Nearctic and Palearctic ecozones, implying a potentially older, Pangaean origin of the higher Pselaphinae as a whole. Here, I describe fossils from mid-Cretaceous (~99 million years old) Burmese amber that confirm the existence of crown-group higher pselaphines on the Eurasian supercontinent prior to contact with Gondwanan landmasses. *Protrichonyx rafifrons* **gen. et sp.n.** is placed *incertae sedis* within the higher Pselaphinae. *Boreotethys* **gen.n.**, erected for *B. grimaldii* **sp.n**. and *B. arctopteryx* **sp.n.**, represents an extinct sister taxon and putative stem group of Bythinini, a Recent tribe with a primarily Holarctic distribution. The Laurasian palaeolocality of the newly described taxa implies that higher pselaphines are indeed probably of Jurassic, Pangaean extraction and that the Laurasian-Gondwanan tribal dichotomy of this clade may have developed vicariantly following Pangaean rifting. Higher pselaphines probably predate the earliest ants. Their physically protective morphological ground plan may have been a preadaptation for myrmecophily when ants became diverse and ecologically ubiquitous, much later in the Cenozoic.

This published work has been registered in ZooBank, http://zoobank.org/urn:lsid:zoobank.org:pub:36E3FE2A-B947-422D-89CA-0EF43B99C382.

Introduction

Pselaphine rove beetles comprise an enormous clade of minute (typically 1–3 mm long), litter-dwelling predators (Chandler, 1990, 2001), currently ranked as the second largest subfamily of Staphylinidae (9854 described species, representing perhaps 10% of the total number of living species). The group reaches peak diversity in tropical forest floors where the beetles achieve high abundance (Olson, 1994; Sakchoowong *et al.*, 2007), suggesting an ecologically important role in litter arthropod communities. Beyond their species richness and ecological success, pselaphines have undergone extraordinary morphological diversification (Raffray, 1890a, 1908; Jeannel, 1954, 1959; Chandler, 2001), displaying dramatic variation in adult structures, to the extent that unambiguous characters for resolving the group's internal relationships have not been forthcoming (Newton & Thayer, 1995; Chandler, 2001). A prominent evolutionary trend also pervades the subfamily: numerous pselaphines in a variety of tribes are social insect inquilines, typically living as socially parasitic myrmecophiles inside ant colonies (or, less frequently, as termitophiles inside termite colonies) (Park, 1942, 1964; Kistner, 1982; Chandler, 2001; Parker & Grimaldi, 2014;

Correspondence: Joseph Parker, Department of Genetics and Development, Columbia University, College of Physicians & Surgeons, 701 West 168th Street, New York, NY 10032, U.S.A. E-mail: jp2488@columbia.edu

Conflict of interest: The author declares no conflict of interest.

Parker, 2016). Inquilinous species range from opportunistic nest intruders (e.g. Park, 1933, 1964) to obligate, morphologically specialized guests that are behaviourally integrated into the social organization of host colonies (Donisthorpe, 1927; Park, 1932; Akre & Hill, 1973; Cammaerts, 1974, 1992; Leschen, 1991).

Factors underlying the diversification and ecological rise of this vast group, as well as its evolutionary predisposition to inquilinism, are not intuitive. Pselaphines are placed within Staphylinidae (Newton & Thayer, 1995), itself the largest family of beetles with more than 61 000 described species (A. Newton, personal communication). Yet, a fundamental difference in morphology between pselaphines and most other rove beetles implies that pselaphine diversification may be a phenomenon largely separate from the success of the majority of this family. The typical staphylinid body form – shortened elytra exposing a narrow, flexible abdomen composed of telescoping segments – permits rapid undulation through substrates and is a morphological innovation that probably facilitated the group's proliferation in soil and litter microhabitats (Hammond, 1979; Newton & Thayer, 1995; Hansen, 1997). Pselaphines, by contrast, have abandoned this apparently adaptive body plan; they too possess similarly short elytra, but their abdominal segments are relatively inflexible, and the entire body is often more compact with a heavily sclerotized integument. Pselaphines have thus radiated impressively in litter despite replacing body flexibility with a more rigid and robust overall frame.

Comprehending the success of Pselaphinae depends on resolving the group's phylogeny, as well as inferring a realistic time frame for its cladogenesis using information from the fossil record. To date, no comprehensive phylogenetic analysis of the 39 tribes of Pselaphinae has been published. The only study to consider explicitly the entire subfamily's internal relationships at any level is that of Newton & Thayer (1995), in a morphological analysis that formally established Pselaphinae as a subfamily of Staphylinidae (reduced in rank from its former status as the family Pselaphidae, and placed in the 'omaliine group' of staphylinid subfamilies). In that work, the former pselaphid subfamilies were reduced to seven 'supertribes', but the monophyly of most of these, as well as the relationships between them, remained largely tentative. Despite this lack of internal resolution, Newton & Thayer's study identified one important and well-supported relationship: the basal split in Pselaphinae between the supertribe Faronitae, and the remaining Pselaphinae (herein termed the 'higher Pselaphinae'). This basal split (Fig. 1) has now been confirmed molecularly in a large-scale, taxonomically comprehensive multilocus phylogeny of all tribes and subtribes of Pselaphinae (J. Parker, unpublished data).

The Faronitae–higher Pselaphinae split may be key to understanding why pselaphines have been so successful, because it appears to mark a fundamental transition in the subfamily's evolution. Faronitae are a relatively small group (291 species), with members that retain a plesiomorphic, more elongate and relatively flexible staphylinid-like body plan. The supertribe is largely excluded from the tropics (Chandler, 2001), and contains no known inquilines. In contrast, the higher Pselaphinae is a vast, tropically dominant clade, where the body plan departs the ancestral staphylinid form and assumes the well-known compact, consolidated shape that is typical of most pselaphines. It is within the higher Pselaphinae that all known inquilinous lineages are found, their profusion and taxonomic distribution collectively implying a clade-wide preadaptation to evolving this lifestyle. The distinction between these two principal clades of Pselaphinae is thus a fundamental one, embodying a stark asymmetry in net diversification rate. The higher Pselaphinae, representing >97% of pselaphine species, is where most of the subfamily's modern species richness is held. Inferring when crown-group higher Pselaphinae arose is therefore critical for understanding the time frame of pselaphine diversification and the potential factors that contributed to it.

The present-day zoogeography of the higher Pselaphinae, however, presents a conundrum. The vast majority of its constituent tribes are confined to, or have their highest centres of diversity in, Gondwanan-derived landmasses – a pattern consistent with a Cretaceous, Gondwanan origin of the higher Pselaphinae. However, a handful of tribes are confined principally to the Nearctic and/or Palearctic regions. These Holarctic groups could conceivably have descended from Gondwanan ancestors, but their existence raises an alternative possibility for the age and origin of the higher Pselaphinae. Recent Holarctic groups may represent lineages of Laurasian origin, meaning that the higher Pselaphinae as a whole could be far older, having originated in the Jurassic when the northern and southern supercontinents were united as Pangaea. Until now, however, the fossil record of the subfamily (summarized in Fig. 1) has yielded scarce information about when the higher Pselaphinae might have arisen. The most extensive work on fossil pselaphines is by Schaufuss (1890) and describes specimens in Middle Eocene (Lutetian) Baltic amber, merely revealing that a large number of higher pselaphine tribes had appeared by the Middle Eocene (Fig. 1). Similarly, a recent study by Parker & Grimaldi (2014) reported stem-group Clavigeritae, a clade of specialized myrmecophilous pselaphines deeply embedded within the higher Pselaphinae, in Early Eocene (Ypresian) Cambay amber. In contrast, a recent study of rove beetles in mid-Cretaceous Spanish amber included descriptions of two new pselaphine genera, one of which was tentatively placed in the higher pselaphine tribe Arhytodini (Peris *et al.*, 2014); however, as discussed in detail in this paper, both new taxa are highly plesiomorphic and, in fact, lack autapomorphies of the higher Pselaphinae. Consequently, unequivocal crown-group higher pselaphines have not been documented as occurring prior to the Eocene.

Here, I present fossils in mid-Cretaceous Burmese amber that represent the earliest-known definitive members of crown-group higher Pselaphinae to be described. Their systematic placements are discussed and evaluated phylogenetically in a small, combined morphological and molecular analysis. The fossils confirm the presence of higher Pselaphines on Eurasia prior to its suturing with Gondwanan landmasses. Together with the Gondwanan bias evident in the contemporary zoogeographic distribution of most higher pselaphine tribes, the Burmese fossils support the hypothesis that this giant clade originated during the late Jurassic at the latest. Vicariance caused by Pangaean breakup is posited to explain why many Recent tribes have a

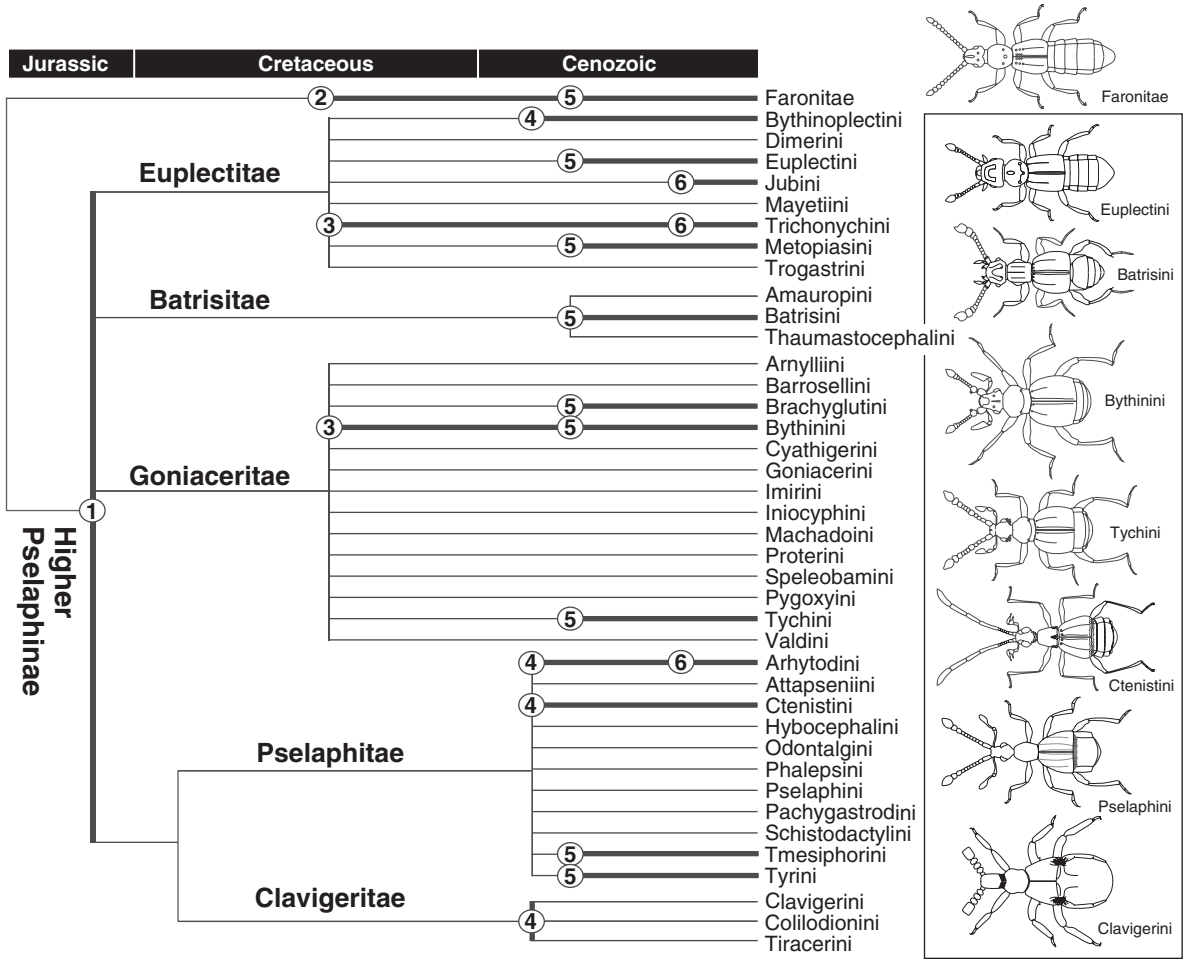

Fig. 1. Current knowledge of Pselaphinae relationships and fossil record. Cladogram based on supertribal relationships of Newton & Thayer (1995) with the inclusion of the former Bythinoplectitae within Euplectitae following Chandler (2001). Habitus outlines of Faronitae and some tribes of higher Pselaphinae (boxed) are shown on the right. Internal relationships in the higher Pselaphinae follow the prevailing view but are not endorsed by the author, and will change dramatically on an impending phylogenetic analysis. Thick branches and numbers indicate inferred minimum ages of taxa based on: (1) inferred minimum age of higher Pselaphinae (this study); (2) inclusions of putative Faronitae in Albian Spanish amber (Peris *et al.*, 2014); (3) inclusions of trichonychine-like Pselaphinae and stem Bythinini in Cenomanian Burmese amber (this study); (4) inclusions of Arhytodini, Ctenistini, Bythinoplectini and stem group Clavigeritae in Ypresian Cambay amber (Parker & Grimaldi, 2014); (4) specimens of multiple tribes in Lutetian Baltic amber (Schaufuss, 1890); (6) Jubini, Trichonychini and Arhytodini in Dominican amber (specimens in AMNH collection, J. Parker, personal observation).

Laurasian or Gondwanan bias. I review the state of knowledge of Cretaceous Pselaphinae and reassess the placements of two previously published fossils. Most notably, a compression fossil from the mid-Cretaceous of Australia (Jell & Duncan, 1986; Jell, 2006) – to my knowledge the oldest supposed fossil pselaphine, and a specimen that could support the Pangaean origin of higher Pselaphinae – is morphologically reinterpreted, leaving its identity as a pselaphine uncertain. Given the newly inferred Jurassic age of the higher Pselaphinae, I speculate that the morphological ground plan of this clade may have been initially adaptive for strengthening the body for locomotion through dense substrates and for defence from predators. Later, as ants came to dominate the Cenozoic tropical forest floor, the heavy integument and compact form of many higher pselaphines may have been preadaptive for ecological coexistence in ant-rich habitats and predisposed these beetles to convergently evolve myrmecophily.

Materials and methods

Amber preparation and observation

The amber specimens described in this paper are part of the American Museum of Natural History (AMNH) collection. Extraction and preparation of the amber specimens are described in Grimaldi *et al.* (2002). All inclusions are in thin, trimmed amber fragments that have been epoxy-embedded and polished. For compound microscopy, embedded amber pieces

were slide-mounted with a thin coat of glycerol between the amber and cover slip. A Zeiss Axiocam mounted on a Zeiss compound microscope, with lighting provided from above, was used to capture image stacks in Zen software (Zeiss, New York, NY, U.S.A.). Montage images were produced in HELICON FOCUS or COMBINEZM. Use of a fluorescent light source, combined with a rhodamine filter, was successful in imaging particularly dark regions of specimens that standard lighting failed to adequately illuminate (Figs 2C–E, 3E).

Morphological description

In the descriptions that follow, the terminology of Chandler (2001) is used, including the foveal system, with fovea acronyms used in Chandler (2001) included in parentheses. Note, however, that 'ventrite' is used in place of 'sternite' for the ventral pterothorax following Herman (2013). It should be mentioned that, although desirable for any description of Pselaphinae, thorough assessment of the foveation pattern is difficult for specimens trapped in amber. Foveal positions are commonly obscured by obstructing body parts, gas bubbles, pieces of extraneous material or damage to the specimen. I have endeavoured to note explicitly when foveae cannot be assessed due to their concealed positions, as well as instances where the presence of a fovea is suspected but cannot be reliably confirmed. In replicating specimen data in the descriptions below, separate labels are bounded by '//' symbols, and new lines of text within data labels indicated by '/'. Ink-written text is symbolized with italics.

Confocal microscopy

Specimens were incubated in DNA extraction buffer (recipe in Gilbert *et al.*, 2007), washed in ethanol and then partially disarticulated. Body parts were mounted in Vectashield (Vector Labs, Burlingame, CA, U.S.A.). A Leica SP5 confocal microscope with a 488 nm laser was used to create image stacks that were then maximally projected in LAS AF (Leica, Nußloch, Germany).

Phylogenetic placement of fossil taxa

To evaluate the phylogenetic positions of the amber pselaphines described in this study, a small, combined morphological and molecular analysis was performed incorporating the fossils and an array of Recent taxa. Taxon sampling is documented in Table S1, and included 40 ingroup Pselaphinae representing all six supertribes and a broad range of tribes. In addition, 15 outgroup taxa, spanning the four 'subfamily groups' of Staphylinidae (Lawrence & Newton, 1982), were included, with expanded sampling from the omaliine group in which Pselaphinae are currently placed (Newton & Thayer, 1995). *Scirtes hemisphericus* Linnaeus of the basal polyphagan family Scirtidae (Hunt *et al.*, 2007) was used as a designated outgroup for rooting the topology. As well as resolving placements of the fossil taxa, this analysis also helps to establish some Cretaceous dates for nodes in a forthcoming fossil-calibrated, mulitlocus phylogenetic analysis of Pselaphinae, including ∼240 ingroup Pselaphinae from all tribes (J. Parker, unpublished data).

Morphological data

Fifty-seven adult characters were scored from all species, based on an expanded subset of those used by Newton & Thayer (1995) and Parker & Grimaldi (2014). The final character matrix was constructed in MESQUITE v. 2.75 (Maddison & Maddison, 2011) and is presented in Table 1. Characters are expressed as homology statements following the guidelines of Sereno (2007). Unknown states were coded '?' and inapplicable states '–'. Characters used by Newton & Thayer (1995) are indicated with 'NT_X' where X is the character number in that paper. Apart from characters constructed using segment numbers or relative size/length ratios of structures, references to images or descriptions of other characters not illustrated in the present paper are provided.

Characters

1. **Body, foveation pattern.** Pselaphine pattern of foveation absent (0); foveae present on body in partial or complete pattern depicted in Chandler, 2001, fig. 1 (1).

2. **Body, pubescence.** Without squamous (broad, flattened or sugar crystal-like) pubescence (0); squamous pubescence on at least some body regions (1).

3. H**ind body, width.** Narrow, elytra and abdomen less than 1.5× as wide as pronotum and head, body appearing parallel-sided (0); wide, elytra and abdomen 1.5× or wider than pronotum and head (1).

4. **Hind body, convexity.** Nonconvex, pterothorax, elytra and abdomen dorsoventrally shallow, body appearing flattened in profile, (0); convex, pterothorax, elytra and abdomen deep in the dorsoventral axis, body appearing globular (1).

5. **Mandible, position relative to oral cavity.** Protruding outside oral cavity to at least half mandible length (e.g. Fig. 5B) (0); concealed within oral cavity, at most apical teeth visible in dorsal view (e.g. Parker & Grimaldi, 2014; figure S1A, B) (1).

6. **Mandible, prostheca.** Present (0); absent (1). (NT_34)

7. **Maxillary cardo, shape.** Cardo unmodified in form, not projecting strongly anteriorly (e.g. Fig. 5B) (0); cardo large and projecting strongly anteriorly beyond side of oral cavity (Park, 1942; plate VII, fig. 1) (1).

8. **Maxillary palpus, size.** Extending well outside oral area and easily visible in dorsal view (0); scarcely visible, largely recessed inside buccal cavity (e.g. Parker & Grimaldi, 2014; figure S1A, B) or at least not visible dorsally (1).

9. **Maxillary palpus, segment number.** Four (excluding the apical fifth pseudosegment of Pselaphinae) (0); fewer than four segments (1).

10. **Maxillary palpomere 1, length.** Short, much shorter than palpomere 2, not extending beyond lateral margins of head (0); long, over half the length of palpomere 2 and clearly able to extend beyond lateral margins of head when so orientated (e.g. Chandler, 2001, figs 186–189) (1). Taxa with fewer than four palpomeres were coded as inapplicable.

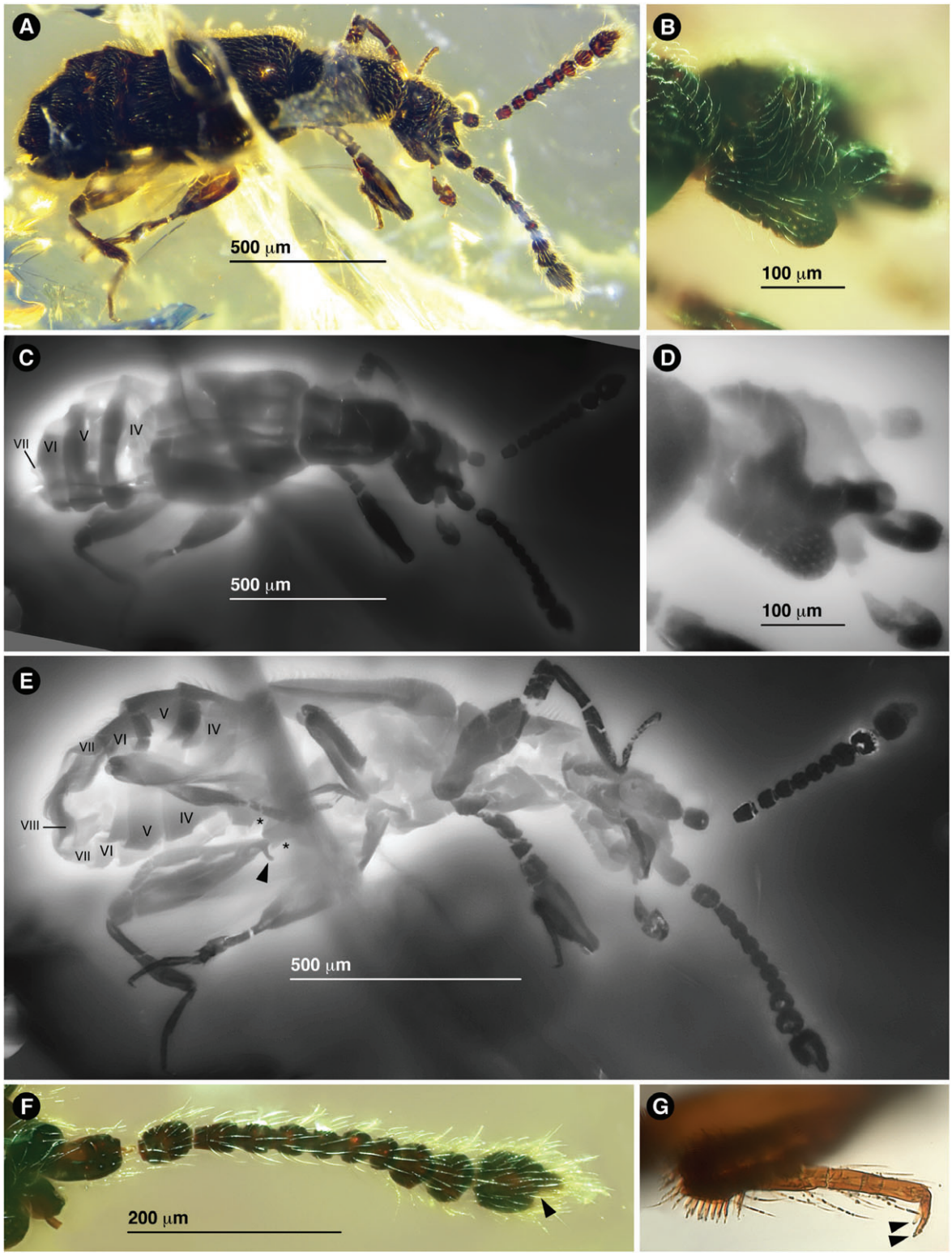

Fig. 2. *Protrichonyx rafifrons* **gen. et sp.n.** AMNH Bu-614. (A, C) Dorsolateral habitus with standard lighting (A) and fluorescent lighting with rhodamine filter (C; tergite numbers labelled). (B, D) Head with standard lighting (B) and fluorescent lighting (D). (E) Ventral habitus with fluorescent lighting, with sternites labelled. Asterisks flank the projecting metacoxa, and the arrowhead indicates the hook-shaped projection of the metatrochanter. (F) Right antenna, arrowhead marks notched apex of terminal antennomere. (G) Right protarsus, with two claws indicated.

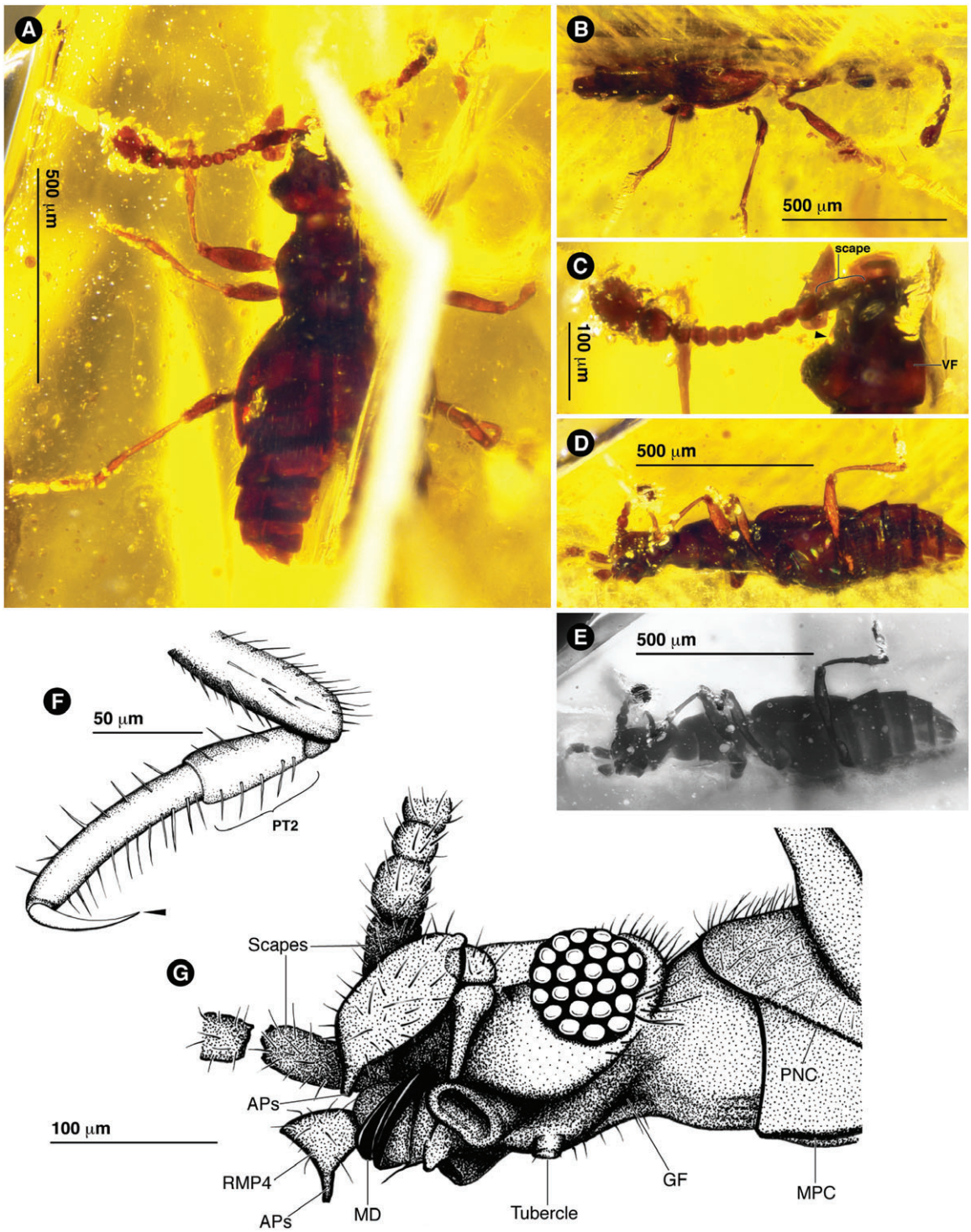

Fig. 3. *Boreotethys grimaldii* **gen. et sp.n.** AMNH B-023. (A) Dorsal habitus. (B) Lateral habitus. (C) Head vertex and appendages; the relatively long scape and right vertexal fovea (VF) are indicated. Arrowhead marks the interrupted ocular mandibular carina. (D) Ventral habitus with standard lighting. (E) Fluorescent lighting with rhodamine filter to reveal sternites. (F) Right protarsus with short protarsomere 2 (PT2) and single claw (arrowhead) indicated. (G) Ventrolateral head to show complexity of gular area and enlarged maxillary palpi. RMP4, right maxillary palpomere 4; APs, apical pseudosegment; MD, mandibles; GF, putative location of gular fovea; PNC, paranotal carina; MPC, putative medial prosternal carina.

Table 1. Morphological character matrix used in phylogenetic analyses.

	1	2	3	4	5
	1	0	0	0	0	0
Adranes taylori	101111011------1001100-0000011000000111001100011101111011
Apharinodes papageno	1111010100000001001100-0010000000010000111100110101111111
Batriscenaulax modestus	1011010000000001110110-1010100010010010111110110011101111
Batrisodes lineaticollis	1011010000000001110110-1010100010010010111110110011101111
Boreotethys arctopteryx	10100??00?10110???01?????110000000?00000??????00?1101111
Boreotethys grimaldii	10100?000?101101?101?0?0111000000001100000?????00011101111
Bryaxis curtisii	1011010000101101011110-0111000100011000001110010001101111
Caccoplectus orbus	1101010100000001011110-0000000110000000001100011101011011
Claviger testaceus	101111011------1001100-0000011000010111001100011101111011
Conoplectus canaliculatus	1001010000000001010110-1010000111011000001110110000001111
Ctenisodes piceus	1111010000010001001100-0010000000010000001100010101111101
Curculionellus sp	1110010001100001001110-0010000000001001000100011101111111
Dasycerus angulicollis	1011000000000000000000-0010000100000000001010100000001000
Dasycerus carolinensis	1011000000000000000000-0010000100000000001010100000001000
Decarthron sp	1011010000000001010101010100100000100100111110110001101111
Endytocera sp	1000011000000001010101100100001100110000011101100000001111
Euaesthetus sp	0000000000000000000000-0000000000000000000-00010000000001
Euplectus piceus	1000010000000001010110-0010000100011000001111110000001111
Eusphalerum luteum	0000000000000000000000-0000000000000000000-10000000000000
Eutyphlus schmitti	1000010000000001010100-1010000110011000001110110000001111
Faronus parallelus	1000010000000001000110-0000000100101000001100110000001001
Glypholoma pustuliferum	0000000000000000000000-0000000000000000000-10000000000000
Harmophorus sp	1011010000000001010110-0010000100001010111110010001101111
Jubus sp	1000011000000001010111100100001100110000011101100000001111
Lasinus mikado	1011010000000001001100-0010100010010000001100011101111101
Leptoplectus pertenuis	1000010000000001010110-0010000000011000001111110000001111
Megarafonus ventralis	1000010000000001000110-0000000100101000001100110000001001
Melba thoracica	1001010000000001010110-1010000100010000001110110000001111
Metopiasini sp	1011010000000001001110-1011000110010000001111110001001111
Metopsia clypeata	0000000000000000000000-0000000000000000000-10000000000000
Micropeplus sp	0000000000000000000000-0000000000000000000-00000000000000
Neophonus sp	0011000000000000000000-0010000100000000001010000000001000
Neuraphes elongatulus	0011000000000000000000-0000000000000000000-00010000000000
Odontalgus sp	1111010000101011001100-0010000000010000011100011101111101
Oropodes chumash	1000010000000001010111010100001100110000011101100000001111
Oxytelus sculpturatus	0000000000000000000000-0000000000000000000-00000000000001
Phloeocharis subtillissima	0000000000000000000000-0000000000000000000-00000000000000
Platystethus arenarius	0000000000000000000000-0000000000000000000-00000000000001
Proteinus brachypterus	0010000000000000000000-0000000000000000000-10000000000000
Protrichonyx rafifrons	?0000?000?000001??011???0100000?001?00000??????00?0001111
Pselaphogenius sp	1110010001101011001110-0011000000010010001000011101111111
Pselaphus heisei	1110010001101011001110-0011000000010010001100111101111111
Pyxidicerina sp	1000010000010001001100-0000000000011000001101110000001011
Reichenbachia juncorum	1011010000000001010101000100000000110100111110010001101111
Rhexius sp	1000010000000001010100-1011000111011000001110110000001111
Rhytus sp	111101011------1001110-0001000100000000001100011101111111
Rybaxis laminata	1011010000000001010101000100001000100100111110010001101111
Sagola sp	1000010000000001000110-0000000100101000001100110000001001
Scirtes hemisphericus	0000000000000000000000-0000000000000000000-00000000000000
Sonoma sp	1000010000000001000110-0000000100101000001100110000001001
Stenichnus collaris	0011000000000000000000-0000000000000000000-00010000000000
Tmesiphorus costalis	1011010000010001001100-0011000000010000001100010101011101
Tychobythinus sp	1011010000101101011110-0111000100011000001110010001101111
Zethopsus sp	1000010000010001001100-0000000000011000001101110000001011

11. **Maxillary palpomere 2, length.** Shorter than one-fifth antenna length (0); approximately equal to or longer than one-fifth antenna length (1). Taxa with fewer than four palpomeres were coded as inapplicable.

12. **Maxillary palpomere 3, shape.** Simple, lacking spines (0); produced into a long, spinose tubercle along lateral margin (Chandler, 2001, fig. 207) (1). Taxa with fewer than four palpomeres were coded as inapplicable. Taxa with fewer than four palpomeres were coded as inapplicable.

13. **Maxillary palpomere 4, length.** Shorter than one-fifth antenna length (0); approximately equal to or longer than one-fifth antenna length (1). Taxa with fewer than four palpomeres were coded as inapplicable.

14. **Maxillary palpomere 4, width.** At most as wide as scape width (0); clearly wider than scape (1). Taxa with fewer than four palpomeres were coded as inapplicable.

15. **Maxillary palpomere 4, elongate peduncle.** Absent, palpomere variously shaped but never lengthily pedunculate (0); present, palpomere lengthily pedunculate with thin, elongate stem and broadening only in apical half (e.g. Chandler, 2001, figs 167, 186–189) (1). Taxa with fewer than four palpomeres were coded as inapplicable.

16. **Maxillary palpomere 5 (apical pseudosegment).** Absent (0); present (1). (NT_37). Taxa with fewer than four palpomeres, all Pselaphinae, still appear to have this structure at the apex of the maxillary palpomere, so were coded 1.

17. **Epipharynx, setal number.** Fewer than four medioapical setae (0); four medioapical setae (Kurbatov, 2007, figs 26–51) (1).

18. **Head, ocular mandibular carina.** Absent (0); present, connecting anterior of eye to lateral margin of oral cavity (Chandler, 2001, p. 28) (1).

19. **Head, frontal rostrum.** Absent or only weakly evident, with front of head broad between widely separated antennal bases that are not mounted on a raised projection between eyes (0); present, with pronounced narrowing of head to clypeus and antennal bases closely approximate, mounted on raised projection between eyes (Chandler, 2001, p. 27) (1).

20. **Head, shelf-like projections**. Absent, base of antennal scape exposed in dorsal view (0); present, base of antennal scape partially obscured from above by a lateroapical protrusion of the frons, with antennae attached to its underside (1). (NT_17). Note that this character is interpreted as distinct from the 'ridge or a shelf-like elevation' of the side of the frons into which the antennae are inserted in (at least some) Oxytelinae (Grebennikov & Newton, 2012) and Scydmaeninae (Grebennikov & Newton, 2009), and these groups were coded as 0.

21. **Vertex, sulcus**. Absent, no declivity on head (0); present, variously shaped impression running from between antennae to between eyes (Chandler, 2001, p. 27) (1).

22. **Gular, longitudinal carina.** Absent (0); longitudinal carina present (Chandler, 2001, p. 29, fig. 1) (1).

23. **Gula, longitudinal carina shape.** Not forked (0); forked, forming V- or Y-shape (Park, 1942, plate VII, fig. 1) (1). Species without longitudinal carina coded as inapplicable.

24. **Gular longitudinal sulcus.** Absent (0); present (Chandler, 2001, p. 29) (1).

25. **Gular modifications in males.** Absent or sometimes gula with median carina or sulcus but never complexly fashioned into tubercles or folds (0); present, with configuration of tubercles, spines or excavations (Fig. 5B, C, E; Löbl & Kurbatov, 1995, figs 1–3) (1).

26. **Antennae, apical club of three segments.** Absent, antennomeres 1–3 not abruptly enlarged relative to preceding segments (0). Present, apical three antennomeres enlarged (1).

27. **Antennal scape, length**. Scape shorter than antennomeres 3–5 combined (0); scape as long as or longer than antennomeres 3–5 combined (1).

28. **Antennal scape, apical notches.** Absent (0); Present, scapes apically indented both dorsally and ventrally (Chandler, 2001, fig. 10) (1).

29. **Antennomere number.** Seven or more (0); six or fewer (1).

30. **Apical antennomere, apex shape.** Rounded or acuminate (0); truncate (Parker & Grimaldi, 2014, figure S1C) (1).

31. **Pronotum, antebasal sulcus or impression.** Absent (0); present (1). (NT_53)

32. **Pronotum, medial longitudinal sulcus.** Absent (0); present (Chandler, 2001, p. 31, fig. 1) (1).

33. **Prosternum, head rest.** Absent, prosternum simple, unmodified to accommodate the head when deflexed (0); present, prosternum and procoxae fashioned into an excavation to receive the head when deflexed (1). The derived state of this character has not, to my knowledge, been illustrated, but is used to distinguish genera of Trogastrini, where the pronotum forms a 'hood' to cover the head in repose.

34. **Elytron, discal foveae.** Absent (fovea may still be present at elytron base) (0); present (e.g. Fig. 7B) (1).

35. **Elytron, sutural stria.** Absent (0); present (1). (NT_70)

36. **Elytron, marginal carina.** Absent (0); present, extending from humerus to at least half elytron length (Chandler, 2001, p. 35: 'marginal stria') (1).

37. **Abdomen, trichomes.** Absent (0); present (Parker & Grimaldi, 2014, figure S1D, E) (1).

38. **Abdominal tergite IV, relative length.** Subequal in length to tergite V (0); at least 1.3 times as long as tergite V (1). In taxa with fused tergites (Clavigeritae), the tergite lengths can still be deduced from the paratergite boundaries.

39. **Abdominal tergites IV–VI, anteroposterior fusion.** Absent, tergite boundaries distinct (0); present, tergites fused into a composite 'tergal plate' (Parker & Grimaldi, 2014, figure S1A) (1).

40. **Abdominal tergites and sternites IV–VI, dorsoventral fusion**. Absent, tergites separated from corresponding sternites (0); present, abdominal margins fully sclerotized via fusion of tergites to corresponding sternites (paratergites absent, or paratergal lines indicated only by carinae) (Nomura, 1991, figs 41E, 44A) (1).

41. **Sternite III, length.** Long, extending past metacoxal apex (Chandler, 2001, fig. 16) (0); short, visible only between metacoxae, if visible at all (Chandler, 2001, fig. 12) (1).

42. **Abdominal sternites III and IV, basal sulcus.** Absent (0); present, apex of sternite III/ base of sternite IV shaped into a deep transverse sulcus (1). (NT_88)

43. **Abdominal sternites III and IV, basal sulcus setal concentration.** Basal sulcus setose (0); sulcus nude (1). Species without longitudinal carina were coded as inapplicable. (NT_89)

44. **Abdominal sternite VIII, defensive gland.** Absent (0); present (1). (NT_92)

45. **Abdominal genital aperture in males.** Formed by apical sternite and tergite, and opening in dorsoventral plane (0); formed by medially bisected sternite VIII with left and right halves (halves may be unequal in size), and opening in lateral plane (Chandler, 2001, p. 36, fig. 13) (1).

46. **Aedeagus, symmetry.** Median lobe and parameres symmetric (0); median lobe and/or parameres asymmetric (1).

47. **Procoxal fissure**. Open, protrochantins partly visible ventrolaterally (0); closed, protrochantins concealed (1). (NT_56)

48. **Protrochanter, length of dorsal margin.** Short, profemur base nearly touching procoxa apex (0); long, clearly longer than protrochanter width, so profemur base and procoxa apex widely separated (1). [NT_84 describes this character for the mesotrochanters; here it is applied to the protrochanter (character 49) and metatrochanter (character 53) also].

49. **Mesotrochanter, length of dorsal margin.** Short, mesofemur base nearly touching mesocoxa apex (0); long, clearly longer than mesotrochanter width, so mesofemur base and mesocoxa apex widely separated (1). (NT_84; see character 48 for further description of this character).

50. **Metathoracic medioapical fovea.** Absent, intercoxal area between metacoxae simple (0); present (Chandler, 2001, p. 254) (1).

51. **Metacoxae, separation.** Contiguous or nearly so, with at most a narrow acuminate intercoxal process (0); widely separated by broad intercoxal process (1). (NT_66)

52. **Metacoxae, shape.** Projecting posteriorly at articulation with metatrochanter (0); metacoxae not projecting (Chandler, 2001, p. 33) (1).

53. **Metatrochanter, length of dorsal margin.** Short, metafemur base nearly touching metacoxa apex (0); long, clearly longer than metatrochanter width, so metafemur base and metacoxa apex widely separated (1). (NT_84; see character 48 for further description of this character).

54. **Tarsomere, number.** Four or five (0); three (1). Note that Bythinoplectini (and Dimerini and Mayetiini, not included in this analysis) appear to possess only two tarsomeres, but in fact the first tarsomere is present as a diminutive vestige attached to tarsomere 2 (see Coulon, 1989, p. 31, fig. 15).

55. **Tarsomere 2, relative length.** Approximately the same length as tarsomere 1 (0); clearly longer than tarsomere 1 (1). (NT_83)

56. **Posterior tarsal claw, size.** Equal in size to anterior tarsal claw (Chandler, 2001, fig. 20) (0); smaller than anterior tarsal claw, or setiform, or absent (Chandler, 2001, figs 21–23) (1).

57. **Empodial setae.** Present (0); absent (1).

Molecular data

The 57 morphological characters used for placing the new fossils include many that have historically been used for defining higher-level groupings within Pselaphinae (Park, 1942, 1951; Jeannel, 1950a, 1955; Chandler, 2001; e.g. Raffray, 1890b). However, because phylogenetic information for the subfamily is limited, it remains unclear to what extent many of these characters are homoplasious. In an effort to circumvent a possible problem of using such characters in a phylogenetic analysis, a small amount of molecular data was included from the 28s ribosomal RNA gene that I have found to be phylogenetically informative in pselaphines. Although only a single gene fragment of 650–800 bp, this region has proven useful for resolving some important tribal-level relationships in Pselaphinae (e.g. Parker & Maruyama, 2013); this solitary gene region gives an estimation of the entire Pselaphinae phylogeny that gives a similar topology to a multilocus analysis using 4.5 kb of sequence data (J. Parker, unpublished data). Because of its empirical utility, this gene region was employed as an additional source of data, with the aim of strengthening the phylogenetic signal when the datasets were combined. DNA was extracted from Recent taxa using a nondestructive protocol described in a previous study (Parker & Grimaldi, 2014), involving a sodium dodecyl sulphate/proteinase-K-based buffer (Gilbert *et al.*, 2007). The 28s region was amplified with primer pair 28sDD (5′-GGGACCCGTCTTGAAACAC) and 28sFF (5′-CACACTCC TTAGCGGAT) (Hillis & Dixon, 1991), and sequenced using the services of Macrogen Corp. (New York, NY, U.S.A.). New sequence data were compiled with previously published 28s sequences of Pselaphinae (Parker & Grimaldi, 2014), and five additional outgroup sequences from GenBank. Accession numbers are listed in Table S1.

Phylogenetic analysis

Partial 28s rRNA sequences were aligned using MAFFT (Katoh & Standley, 2013) with default parameters, and the alignment minimally edited for obvious errors in Se-Al (Rambaut, 1996); no attempt was made to edit or excise length-variable regions, because, in various trial runs, doing so was found to have negligible impact on the topology of the Pselaphinae tree or branch support values. Model selection in JMODELTEST2 (Darriba *et al.*, 2012) yielded the GTR + I + G model. The Mkv + G model (Lewis, 2001) was specified for the morphological data. For the main analysis, partitioned Bayesian analysis was performed on the combined data, using MRBAYES 3.2.3 (Ronquist *et al.*, 2012) via the Cipres Science Gateway (Miller *et al.*, 2010). Search consisted of two Markov chain Monte Carlo (MCMC) runs of four chains and was terminated at two million generations. Convergence was determined by the standard deviation of split frequencies having dropped below 0.0075, and further verified by estimated sample sizes higher than 200 in TRACER (Rambaut *et al.*, 2013), indicating sufficient estimation of the posterior. The first 25% of trees were discarded as burn-in. The consensus tree of both MCMC runs was rooted using *Scirtes*

hemisphericus (Scirtidae). The nexus file used for this combined analysis is available in File S1. In addition, separate analyses were also performed of the morphological and molecular partitions to gauge how combining the two datasets had affected the topology of the primary analysis. Finally, parsimony analyses of the combined and separate data partitions were carried out using TNT (Goloboff *et al.*, 2008). The commands 'mult = tbr replic 10 000 hold 1000 ratchet drift;' were used for tree search. Clade support was tested via bootstrap (Felsenstein, 1985) with 'resample boot replic 1000'. All characters were treated as unordered multistate.

Age and palaeoenvironment

The Burmese amber specimens described herein were extracted from deposits in Kachin state, northern Myanmar. Radiometric dating has yielded a maximal age of Burmese amber of 98.79 ± 0.62 Ma (Shi *et al.*, 2012), corresponding to earliest Cenomanian (Ogg *et al.*, 2012). Based on the taxonomic diversity of invertebrates in Burmese amber, the palaeoenvironment in which it formed has been hypothesized to be moist tropical forest, with conifers of the families Cupressaceae (Grimaldi *et al.*, 2002) and Pinaceae (Dutta *et al.*, 2011) thought to be potential sources of the resin itself.

Systematic palaeontology

Family Staphylinidae
Subfamily Pselaphinae Latreille, 1802
Tribe Incertae sedis

***Protrichonyx* gen.n.**
http://zoobank.org/urn:lsid:zoobank.org:act:DDEF7ED2-68C8-4811-8641-960369D2B6E4

Type species. Protrichonyx rafifrons **sp.n.** here designated.

Diagnosis. Protrichonyx and its single species *P. rafifrons* possess characters typical of the tribe Trichonychini (see 'Systematic placement' later). *Protrichonyx* can be separated from all other trichonychine genera by the following combination of characters: (i) the distinctive quadrate head, with raised vertex, deeply excavate frons produced anteriorly into a wide, shelf-like interantennal bridge, and with basolateral margins that are continuous with the eyes; (ii) apically notched 11th antennomeres; (iii) putative absence of antebasal or medial sulci on the pronotum; (iv) pronotum longer than wide.

Description. Body length ∼1.5 mm (Fig. 2A, C). Form flattened and relatively linear and parallel-sided, with body only moderately broadened behind pronotum.

Head (Fig. 2*B, D):* approximately quadrate, slightly wider than long. Vertex raised behind eyes into transverse arc; region of vertex anterior to arc formed into deep frontal excavation, flanked laterally by raised and widely separated antennal tubercles. Frontal excavation demarcated anteriorly by raised, relatively flat, broad interantennal bridge. Antennal sockets positioned on underside of shelves of raised antennal tubercles (Fig. 2D). Posterior face of raised transverse vertexal arc sloping steeply (Fig. 2D). Eyes prominent on ventrolateral margins of head. Basolateral margins of head straight and seamlessly continuous with eyes, narrowing gradually to occiput. Antenna (Fig. 2F) with 11 antennomeres, with antennal club formed by antennomeres 9–11. Antennomere 11 with notched apex. Three maxillary palpomeres (presumably 2, 3 and 4) visible in the holotype specimen. Gular region damaged by compression or stretching during fossilization (Fig. 2E).

Thorax: pronotum (Fig. 2A, C) ∼1.4× wider than long, approximately equal in width to head. Damage to the pronotum prevents a definitive assessment, but there is no evidence of either an antebasal or median sulcus, and these structures are presumed to be lacking (the transverse line across the pronotum in Fig. 2C is a crack in the cuticle). Prosternal region anterior to procoxae longer than wide. Pterothorax ∼1.5× longer and ∼1.7× broader than prothorax. No assessment can be made of the ventral foveation pattern of the specimen due to its preservation.

Abdomen: dorsal abdomen (Fig. 2C) slightly longer than wide, ∼0.9× elytral length. Abdomen dorsoventrally flattened, and with lateral margins broadly rounded. Segments telescoping, with apical margin of each sclerite overlapping the base of the following sclerite. Five tergites (IV–VIII) visible (Fig. 2C, E), with putative paratergites visible on tergites IV and V. Tergite IV widest and slightly longer than V, with lateral margins narrowing to base. Tergites V–VII sequentially narrowing to abdomen apex. Five sternites (IV–VIII) visible (Fig. 2E), sternite IV longest. Penial plate not apparent.

Elytra: ∼1.2× as wide as long (Fig. 2C), at widest point ∼1.7× wider than base of pronotum. Elytra with humeri smoothly rounded, and with lateral margins relatively straight but broadening gradually to apices. Elytra without clear evidence of striae (longitudinal sulcus-like depressions in Fig. 2C are probably crushing artefacts associated with fossilization). A single basal elytral fovea (BEF in Chandler, 2001) may be positioned on each elytron close to the suture.

Legs: coxal pairs of all legs contiguous. Metacoxae projecting posteriorly (Fig. 2E; see asterisks flanking the left metacoxa). Trochanters short ('brachysceline' type) with minimal distance separating coxa from base of femur. Tarsi three-segmented. Tarsomere 1 short; tarsomeres 2 and 3 subequal in length, each at least 3× longer than tarsomere 1. Tarsi with single, primary claw and at least protarsus with smaller accessory (anterior) claw, which is inconspicuous or absent from meso- and metatarsi (Fig. 2G). Alternatively interpreted as tarsi with single tarsal claws, but protarsal claw longitudinally bifid.

Etymology. The generic name combines the Greek *πρό* ('pro', meaning before) and '*Trichonyx*' Reichenbach, type genus of Trichonychini – the tribe that embodies the plesiomorphic ground plan of the higher Pselaphinae. The gender is masculine.

Comments. The holotype of *P. rafifrons* is the sole specimen of this species and genus and has been subjected to compression or stretching, evident in numerous cracks throughout the specimen (especially clear in Fig. 2E). Damage to the head precludes description of gular morphology, but the morphology of the vertex, with raised transverse arc and frontal excavation, appears to be a genuine morphological feature of this genus and species.

Systematic placement. Protrichonyx presents a suite of characters that would lead to its placement in the supertribe Euplectitae, a group of eight tribes that share a number of character states that are primitive in Pselaphinae. The euplectite body form is typically more flattened, elongate and parallel-sided than most pselaphines (Fig. 2A), the metacoxae are contiguous and project posteriorly (Fig. 2E), and the trochanters of all legs are short, with minimal separation between the apex of the coxa and base of femur ('brachysceline' type). Such states are seen in many outgroup staphylinid subfamilies as well as the plesiomorphic Faronitae, but Euplectitae can be separated from these by some derived features: though relatively parallel-sided and elongate, the euplectite body is generally more compact (and often much smaller), with the trunk and antennal segments more consolidated and less flexible than in Faronitae; the antennae bear a three-segmented club (Fig. 2F); the second tarsomeres are much longer than the first tarsomeres (Fig. 2G); and in most tribes the tarsal claws are unequal in size (Fig. 2G), or reduced to just a single claw. As a group, Euplectitae lack autapomorphies and are not defensibly monophyletic. Instead, the supertribe can be interpreted as embodying the plesiomorphic ground plan of the higher Pselaphinae, and may consequently be paraphyletic with respect to all other nonfaronite Pselaphinae. Monophyly of most of the tribes of Euplectitae, however, is probable on the basis of autapomorphies, but the largest tribe, Trichonychini, is defined by the absence of such characters and is doubtfully monophyletic. *Protrichonyx* has a generalized euplectite morphology and cannot be linked to any of the more derived, putatively monophyletic tribes; *a priori*, *Protrichonyx* would thus be placed into Trichonychini.

Inclusion of *Protrichonyx* in a combined morphological and molecular analysis (Fig. 6B) places it inside the higher Pselaphinae, as one lineage of a polytomy comprising mostly euplectite taxa representing the tribes Jubini, Euplectini, Trogastrini, Metopiasini and part of Trichonychini, and within which the supertribe Batrisitae is also embedded. Support for this placement is relatively weak [posterior probability (PP) = 0.82 for the branch leading up to the polytomy; Fig. 6B], but a position for *Protrichonyx* within this clade is fully consistent with its *a priori* placement in Euplectitae: Trichonychini. Note, however, that the euplectite clade to which *Protrichonyx* belongs does not form a monophyletic group with the remaining Euplectitae included in the analysis (taxa representing the tribe Bythinoplectini, and the trichonychine genus *Oropodes*) (Fig. 8). This inferred fragmentation of euplectite relationships, which is congruent with (and more strongly supported by) a much more taxonomically comprehensive, mulitlocus analysis (J. Parker, unpublished data.), confirms that neither Euplectitae nor Trichonychini are monophyletic. Hence, despite the *a priori* temptation to place *Protrichonyx* within Euplectitae: Trichonychini, both supertribe and tribe should rightfully be dismantled, and I therefore refrain from placing *Protrichonyx* in either. Instead, *Protrichonyx* is placed *incertae sedis* within the higher Pselaphinae, pending a more thorough resolution of euplectite and trichonychine relationships.

Protrichonyx similarly emerges within the higher Pselaphinae when morphology alone is analysed (Fig. 6A). Again, the genus is part of a polytomy with other euplectite taxa that in this case form a basal, paraphyletic 'euplectite grade' to the remaining higher Pselaphinae supertribes (Batrisitae, Goniaceritae, Pselaphitae and Clavigeritae). The euplectite grade in this analysis is probably an artefact of the lack of morphological autapomorphies of Euplectitae, but also stems from the derived morphological character states of non-euplectite higher Pselaphinae constraining these taxa into monophyly. While it is true that Euplectitae have no known autapomorphies, it is probably not the case that the derived states of non-euplectite higher taxa have evolved only once. Indeed, analysis of molecular data alone (Figure S1A) reveals that Euplectitae is paraphyletic with regard to Batrisitae and, independently, paraphyletic also to two groups of Goniaceritae (Bythinini and the brachyglutine genera *Rybaxis*, *Reichenbachia* and *Decarthron*). This result is also seen in the combined analysis (Fig. 6B), revealing that the addition of the minimal 28s region has overcome some of the homoplasy in the morphological data, yielding what is probably a superior estimation of the position of *Protrichonyx*. When all tribes of Pselaphinae are analysed molecularly, the instances of euplectite paraphyly increase further, and indeed the Euplectitae can be seen to arrange into a 'backbone' of the higher Pselaphinae, repeatedly having spawned more derived taxa that are currently placed into the four supertribes Batrisitae, Goniaceritae, Pselaphitae and Clavigeritae, all but the last of which are themselves of doubtful monophyly (J. Parker, unpublished data; aspects of the nonmonophyly of these more derived groups are evident in Fig. 6B and Figure S1A, in the poly/paraphyly of the few included members of Pselaphitae and Goniaceritae).

The outcomes of the three Bayesian analyses are broadly congruent with those of corresponding parsimony analyses in the key placement of *Protrichonyx* in the higher Pselaphine, and its relationship to Euplectitae (Figure S1B–C; note that branch support values are generally weaker in all such parsimony analyses). Additionally, the argument for nonmonophyly of Euplectitae is supported by parsimony analysis of the molecular data alone (Figure S1D).

***Protrichonyx rafifrons* sp.n.**

http://zoobank.org/urn:lsid:zoobank.org:act:0C698F2C-0534-424B-8333-0005CAEFBF60

Type material. Holotype (sex unknown, possible male). 'AMBER: MYANMAR (BURMA)/Upper Cretaceous/Kachin: Tanai Village (on Ledo Rd 105 km NW Myitkyna)/coll. Leeward Capitol Corp., 2000/AMNH Bu-614. // *Pselaphinae* Det.

Chatzimanolis 2012 // Burmese amber: 1 COLEOPTERA.' Specimen in AMNH.

Diagnosis. As for genus.

Description. Body length 1.49 mm (Fig. 2A, C). Colour dark reddish brown with appendages somewhat lighter, (although the extent of body darkening may be a fossilization artefact). Dorsum covered in relatively dense, erect yellow setae.

Head: length 0.22 mm (Figs 2B, D); estimated width across eyes 0.25 mm (note that because of the beetle's orientation in the amber piece, this and all subsequent width figures are approximations). Dorsal head covered with erect yellow setae. Eyes with an estimated 40–50 facets. Antennal length 0.6 mm (Fig. 2F). Antennomere 1 rounded-cylindrical in shape, twice as wide as long. Antennomere 2 rounded-cylindrical, 0.6× antennomere 1 length and slightly narrower. Antennomere 3 obconical, 0.75× antennomere 2 length and slightly narrower. Antennomeres 4–8 equal in width to antennomere 3, approximately globular, and with lengths becoming sequentially slightly shorter. Antennal club formed from enlarged, roughly globular antennomeres 9 and 10 and conical antennomere 11. Antennomere 11 twice as long as 10, tapering to apex but deeply notched in apical third of one face (Fig. 2F, arrowhead; whether the mesial or lateral face is notched cannot be determined due to fixed orientation of the specimen). Estimated length of extended maxillary palpus 0.21 mm. Putative palpomere 2 elongate and broadening apically; palpomere 3 short, approximately triangular in shape; palpomere 4 approximately ovoid.

Thorax: pronotum (Fig. 2C) 0.34 mm long, approximate width at base 0.22 mm. Lateral pronotal margins relatively straight and parallel, widening slightly at base. Pronotum and lateral regions of prosternum covered in thick, long, erect yellow setae. Meso-metaventrite lacking detectable setation.

Abdomen: Dorsal abdomen length along midline 0.45 mm (Fig. 2C). Width at widest point (along apical margin of tergite IV) 0.38 mm. Tergites and sternites covered with raised, posteriorly directed yellow setae. Basal sulcus-like impressions of tergites IV and V (seen in Fig. 2C) may be fossilization artefacts.

Elytra: elytral length along suture 0.48 mm (Fig. 2C). Combined elytral width along apical margin 0.3 mm. Setation on elytra matching the form and density of the pronotum (Fig. 2A).

Legs: metatrochanter with conspicuous hook-shaped projection (Fig. 2E, arrowhead, suggesting the specimen may be male). Femur somewhat thickened, but thickening may be exaggerated by compression during fossilization. Femur and tibia lacking cuticular modifications. Tibia with concentrations of thick setae at apex, most pronounced on protibia (Fig. 2G). Lengths of leg segments: profemur 0.42 mm, protibia 0.32 mm, protarsus 0.19 mm, mesofemur 0.39 mm, mesotibia 0.33 mm, mesotarsus 0.18 mm, metafemur 0.41 mm, metatibia 0.34 mm, metatarsus 0.23 mm.

Etymology. The specific name is a combination of *ράφι* ('ráfi', meaning shelf or rack), and frons, on account of the prominent, raised interantennal bridge forming a transverse shelf spanning the front of the head.

Tribe Bythinini

***Boreotethys* gen.n.**
http://zoobank.org/urn:lsid:zoobank.org:act:BF806B3A-5077-4B2B-BB16-64D84B019B29

Type species. Boreotethys grimaldii **sp.n.** here designated.

Diagnosis. Boreotethys can be distinguished from all other Pselaphinae by the following combination of features: (i) Antennomere 1 elongate, approaching length of, or longer than, antennomeres 3–5 combined; (ii) Maxillary palpus long, equal to or greater than half antenna length, with thin, elongate palpomere 2, small, triangular palpomere 3 and enlarged, roughly elongate-ovoidal palpomere 4; (iii) metacoxae only narrowly separated from each other; (iv) mesotrochanter short (brachysceline-type); (v) tarsomere 2 much longer than tarsomere 1 but distinctly shorter than tarsomere 3; (vi) single tarsal claws.

Description. Body length ~1 mm (Figs 3A, B, 4A). Body relatively flattened dosoventrally (Fig. 3B) and broadened posteriorly, with elytra and abdomen distinctly wider than head and pronotum.

Head: shape approximately triangular (Figs 3C, 4B), width across eyes ~1.2× length from clypeus to neck. Vertex relatively flat; two vertexal foveae present in the type species *B. grimaldii* (Fig. 3C; absent or obscured in *B. arctopteryx*). Basolateral margins of head straight, equal in length to eyes and narrowing to occipital constriction (Figs 3C, 4B). Head narrowing in front of eyes, with frontolateral margins gently sloping to clypeus. Frontal rostrum weakly developed to absent; antennal bases widely separated by flat to weakly impressed interantennal region. Probable gular fovea present, and gular region complexly modified with raised tubercles of cuticle (Fig. 3G; modifications visible only in *B. grimaldii* – this region obscured by bubbles in *B. arctopteryx*). Antenna 11-segmented (Figs 3C, 4B). Antennomere 1 relatively elongate, equal in length to or exceeding antennomeres 3–5 combined. Antennomere 2 also relatively enlarged, at least half the length of antennomere 1. Antennomeres 3–8 roughly globular and subequal in size. Antennal club formed by enlarged antennomeres 9–11. Maxillary palpus enlarged (Figs 3G, 4B), as long or longer than half antenna length, with elongate palpomere 2, small, rounded-triangular palpomere 3 and expanded, roughly ovoidal palpomere 4. Possible apical pseudosegment 5 visible in the type species *B. grimaldii* (Fig. 3G).

Thorax: pronotum (Figs 3A, 4A) approximately equal in width to head (measured across eyes), and slightly transverse, ~1.2× wider than long; widest in anterior half and with rounded lateral margins. Apical margin ~0.8× as wide as basal margin. Pronotum lacking unambiguous antebasal or medial sulci, but basal half of pronotum apparently modified in at least the type

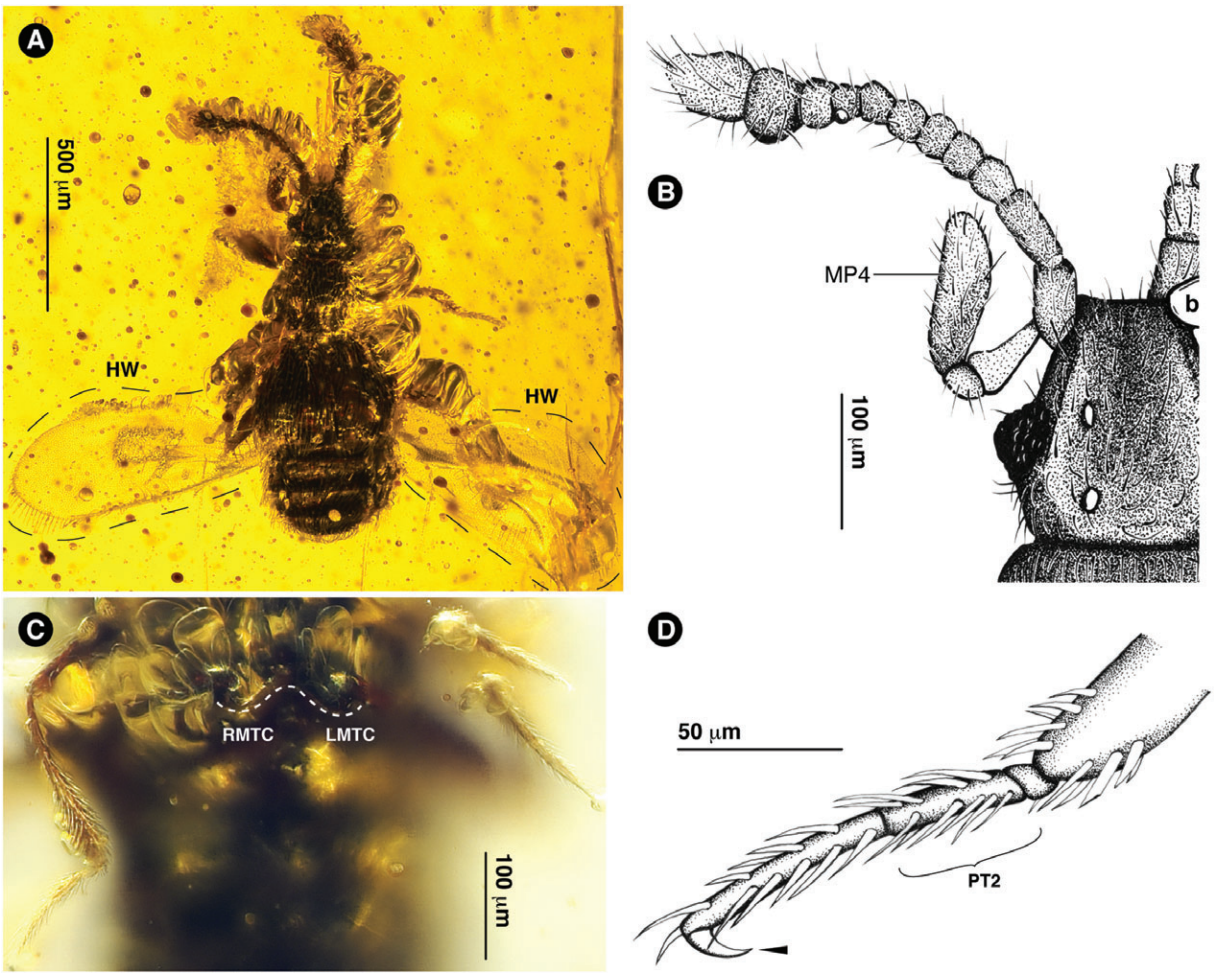

Fig. 4. *Boreotethys arctopteryx* **gen. et sp.n.** AMNH Bu-248. (A) Dorsal habitus with hindwings (HW) outlined. (B) Head vertex and appendages. MP4, maxillary palpomere 4; b, bubble. (C) Metaventral margin with right and left metacoxae outlined (R/LMTC). (D) Right protarsus with short protarsomere 2 (PT2) and single claw (arrowhead) indicated.

species, *B. grimaldii*. The following ventral thoracic foveal characters, seen at angles other than those illustrated, are believed to be diagnostic at the genus level but are based solely on examination of *B. grimaldii*, due to a ventral covering of bubbles in *B. arctopteryx*. Putative lateral procoxal fovea (LPCF) present. Mesoventrite with lateral mesocoxal fovea present. Metaventrite with lateral metaventral fovea (denoted LMTF in Chandler, 2001). Other ventral thoracic fovea not detectable in the holotype of *B. grimaldii*.

Abdomen: Dorsally transverse (Figs 3A, 4A), at widest point 1.3× as wide as long, and approximately equal in width to elytra. Five tergites visible (IV–VIII), tergites IV–VI subequal in length. Margins of tergites IV and V narrowing to their bases; margins of tergites VI–VIII narrowing to their apices. Broad paratergites present on tergites IV–VI; smaller paratergite present on tergite VII. Abdomen ventrally with six sternites (III–VIII) visible. Posterior margin of sternite III entire (Figs 3D, E), uninterrupted by metacoxae. Sternites IV–VII subequal in length; visible (apical) region of sternite VIII much shorter, with basal portion of sternite VIII largely covered by sternite VII.

Elytra: at widest point equal in width to abdomen, and approximately equal in length to abdomen. Lateral margin of elytron smoothly rounded, broadening posteriorly to mid elytral length before narrowing slightly. Posterior margin of elytron broadly arcuate, but lateroapical corner sharply projecting posteriorly (Fig. 3A). Elytron with two possible basal elytral foveae (BEF). Sutural stria present. Marginal carina present on elytron in at least *B. grimaldii*.

Legs: procoxae and mesocoxae contiguous; metacoxae separated by narrow metaventral process. Metatrochanters projecting only weakly posteriorly (Fig. 4C). Mesotrochanters short (brachysceline) with apex of mesocoxa nearly touching base of mesofemur. Tarsi (Figs 3F, 4D) three-segmented. Tarsomeres progressively longer: tarsomere 1 short; tarsomere two 4× as long as tarsomere 1; tarsomere 3 longest, 1.7× as long as tarsomere 2. Single tarsal claws present (arrowheads in Figs 3F, 4D).

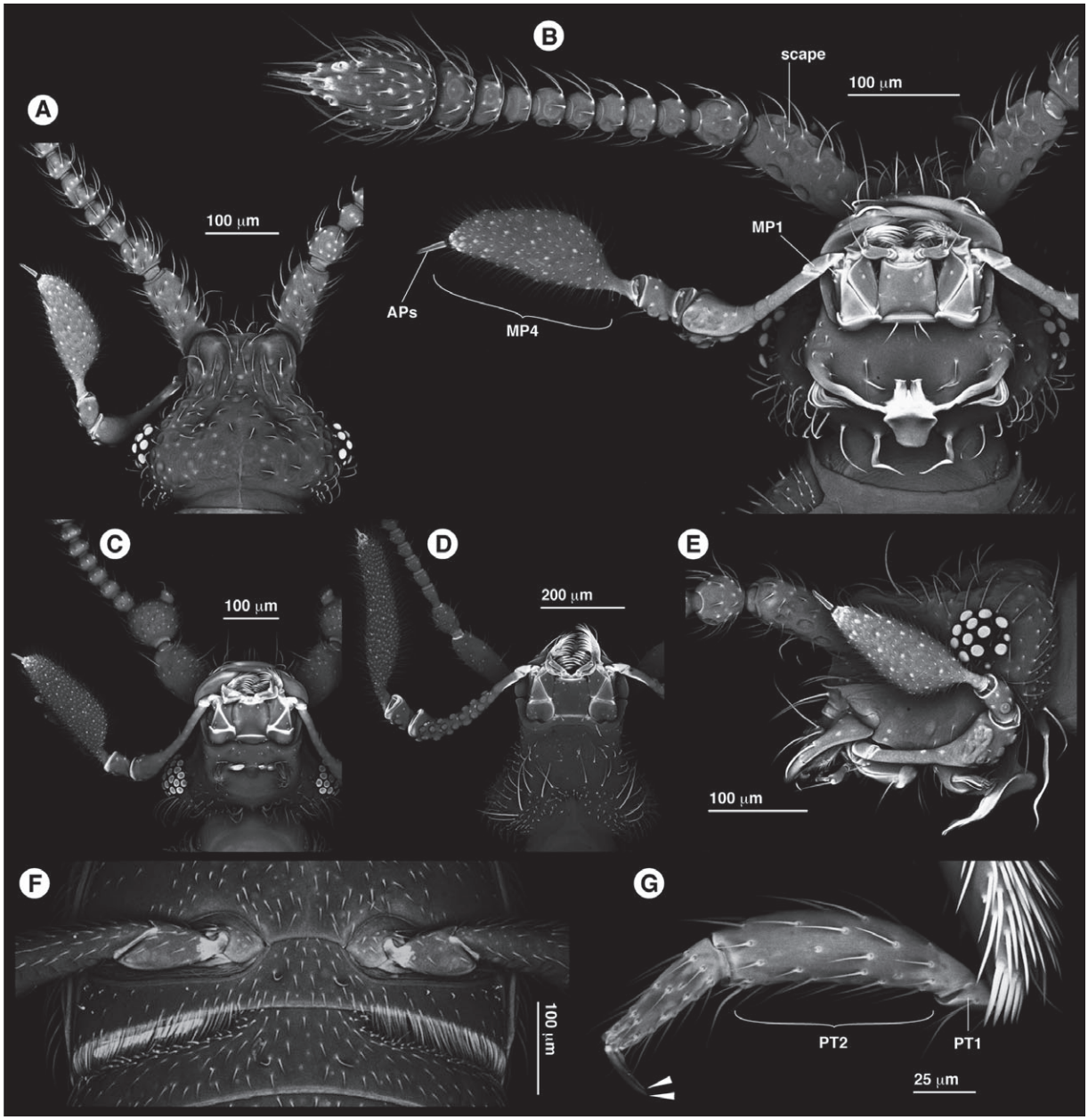

Fig. 5. Confocal reconstructions of Recent Bythinini. (A, B, E) Head of *Tychobythinus* sp. (upstate New York, USA). This large, Holarctic genus is defined by multiple bythinine symplesiomorphies and may approximate the ancestral morphology of crown-group Bythinini (Löbl & Kurbatov, 1995). (A) Vertex showing triangular shape, elongate scapes and enlarged maxillary palpus. (B, E) Underside (B) and lateral view (E) showing complex cuticular modifications. MP1/4, maxillary palpomere 1/4; APs, apical pseudosegment. (C) Modified gular region of *Bryaxis curtisii* (Swansea, UK). (D) Eyeless *Machaerites* sp. (Croatia) with simple gular region but exaggerated, elongate maxillary palpus. (F) Metaventral margin of *Tychobythinus* sp. showing wide metacoxal separation. (G) Protarsus of *Tychobythinus* sp. with tiny tarsomere 1 (PT1), long tarsomere 2 and shorter tarsomere 3. Two unequally sized tarsal claws are present (narrow accessory claw in front partially obscuring broader primary claw behind).

Etymology. The generic name is a combination of the Greek *βόρεια* ('bóreia', meaning 'from the north') and *τηθύς* ('Tethys'), on account of the Laurasian palaeolocality of the amber specimens and their oceanic separation from diverse Gondwanan lineages of higher Pselaphinae. The gender is feminine.

Systematic placement. Boreotethys belongs in the higher Pselaphinae based on a number of derived character states that are not seen in Faronitae: clubbed antennae, metacoxae not strongly projecting posteriorly, second tarsomeres much longer than first tarsomeres, single tarsal claws, and absence of fovea on the elytral disc. Although *Boreotethys* is relatively flat-bodied, its

overall shape and short, broad abdomen are also a departure from the narrow, staphylinid-like body plan of most Faronitae, and approach the archetypal 'compact' higher pselaphine habitus. *Boreotethys* does not obviously belong within the crown-group of any pselaphine tribe, but shares several putative synapomorphies with Bythinini, a largely Holarctic tribe of 27 genera and 612 Recent species. Modern bythinine morphology is depicted in Fig. 5. Members of the tribe are diagnosed by their unique possession of a collection of derived and primitive character states (characters discussed in Park, 1953): (i) enlarged maxillary palpi (derived), which normally measure half the length of the antennae or greater, and comprise elongate second palpomeres, small, approximately triangular third palpomeres and, expanded, typically elongate-ovoidal fourth palpomeres (Figs 5A–D); (ii) antennae often with elongate or enlarged scapes (derived; Figs 5B, D), sometimes also with modified and/or enlarged pedicels, especially in males (Fig. 5C); (iii) males often with a complexly modified gular area with ridges, tubercles, sulci and setae (derived) (see Löbl & Kurbatov, 1995 for a discussion of this character) (Fig. 5B, C, E); (iv) distantly separated metacoxae (derived), which do not project posteriorly (Fig. 5F); (v) single tarsal claws (derived), often with a much smaller secondary claw or seta (Fig. 5G); (vi) short trochanters (primitive), where the base of the femur is in close proximity to the coxa ('brachysceline' type).

Boreotethys possesses the majority of this suite of bythinine characters: similarly enlarged and shaped maxillary palpi (Figs 3G, 4B), antennae with long scapes (Figs 3C, 4B) and long pedicels in *B. arctopteryx* (Fig. 4B), a complexly modified gular region (view unobstructed only in *B. grimaldii*; Fig. 3G), short trochanters on all legs, and single tarsal claws (Figs 3F, 4D). The new genus also has a similar overall habitus to more generalized Bythinini, such as *Tychobythinus* Ganglbauer and *Bryaxis* Kugelann. However, there are notable differences between *Boreotethys* and modern Bythinini. In *Boreotethys*, the body is relatively more flattened than is typical of bythinines, which are dorsoventrally quite convex beetles (a derived condition in Pselaphinae). Furthermore, the metacoxae of *Boreotethys* are more primitively configured: they are not as distantly separated as they are in bythinines, but instead are closer to the ventral midline, although still not contiguous as in Faronitae (the metacoxae are especially close in *B. arctoperyx*; Fig. 4C). A third important discrepancy lies in the length ratio of tarsomeres 1 and 2. In *Boreotethys*, tarsomere 2 is much shorter than tarsomere 3 (Figs 3F, 4D), whereas the opposite is true of modern Bythinini. Such differences are consistent with *Boreotethys* possessing a more plesiomorphic overall morphology than modern Bythinini; *a priori Boreotethys* may therefore represent a bythinine stem group.

Phylogenetic inference of the position of *Boreotethys* within Pselaphinae agrees with this *a priori* notion: the two species emerge together, well inside the higher Pselaphinae, as a sister clade to the included bythinine genera, *Tychobythinus* and *Bryaxis* (Fig. 6). Support for this relationship is maximal, and furthermore is supported by analysis of morphological characters alone (Fig. 6A) and also by parsimony analyses of the combined data (Figure S1D) and morphology only (Figure S1C). I therefore propose that *Boreotethys* is an extinct, Cretaceous stem-group of modern Bythinini. This hypothesis fits well with the biogeographic consistency between *Boreotethys* in Eurasian Burmese amber and the present-day Holarctic range of bythinines. It is important to note, however, that although the two species of *Boreotethys* emerged as sister taxa in all analyses, support for this node was never particularly strong (PP = 0.68 in the combined analysis; Fig. 6B). Indeed, the genus is largely separated from crown-group Bythinini by the absence of some bythinine autapomorphies. It thus remains possible that *Boreotethys* in fact represents a paraphyletic stem 'grade' to Recent Bythinini, although one potential character supporting the reciprocal monophyly of *Boreotethys* and Recent Bythinini is the state of the tarsal claws: in *Boreotethys*, single tarsal claws are present and the accessory claw or seta has apparently been lost (Figs 3F, 4D). In contrast, many modern Bythinini still retain the accessory claw (Fig. 5G) – a more primitive condition. As *Boreotethys* emerges as sister to Bythinini but is not incontrovertibly monophyletic based on present information, I refrain from erecting a new tribe for the genus. Rather, *Boreotethys* is here placed into Bythinini and regarded as an extinct stem-group.

***Boreotethys grimaldii* sp.n.**

http://zoobank.org/urn:lsid:zoobank.org:act:A4760BC0-5DA2-437B-A6FE-C1EEE7889E8B

Bythinini: Parker & Grimaldi (2014), Figure S3B.

Type material. Holotype (sex unknown, putative male). 'AMBER: MYANMAR (BURMA)/Upper Cretaceous?/Kachin: Tanai Village (on Ledo Rd. 105 km NW Myitkyna)/coll. Leeward Capitol Corp., 1999/AMNH B-023. // Burmese amber: COLEOPTERA: Staphylinidae // Burmese amber: 3 COLEOPTERA/1 THYSANOPTERA/*incl. 1 Staphyl.*' Specimen in AMNH.

Diagnosis. Boreotethys grimaldii can be distinguished from its congener, *B. arctopteryx*, in that antennomere 1 is clearly longer than antennomere 2; antennomere 2 is wider than antennomeres 3–8; the metacoxae do not project as strongly as they do in *B. arctopteryx*; the femora are more slender; tarsomere 1 is thicker than tarsomere 2 and the body in general is only sparsely setose.

Description. Body length 1.0 mm (Figs 3A, B). Body slightly shiny; colour uniform light reddish brown, appendages yellow-brown. Most body regions covered in moderate density of short, thin, translucent setae.

Head: length 0.18 mm, width across eyes 0.25 mm (Fig. 3C). Two nude vertexal foveae present, positioned in line with eyes. Vertex with sparse covering of thin, translucent setae. Putative ocular mandibular carina interrupted such that the head capsule anterior to eye appears with short, blunt, triangular process projecting anteriorly; ventrolateral margin of head in front of eye also with blunt triangular cuticular process, the two processes almost meeting (Fig. 3C, arrowhead). Apicolateral angles of

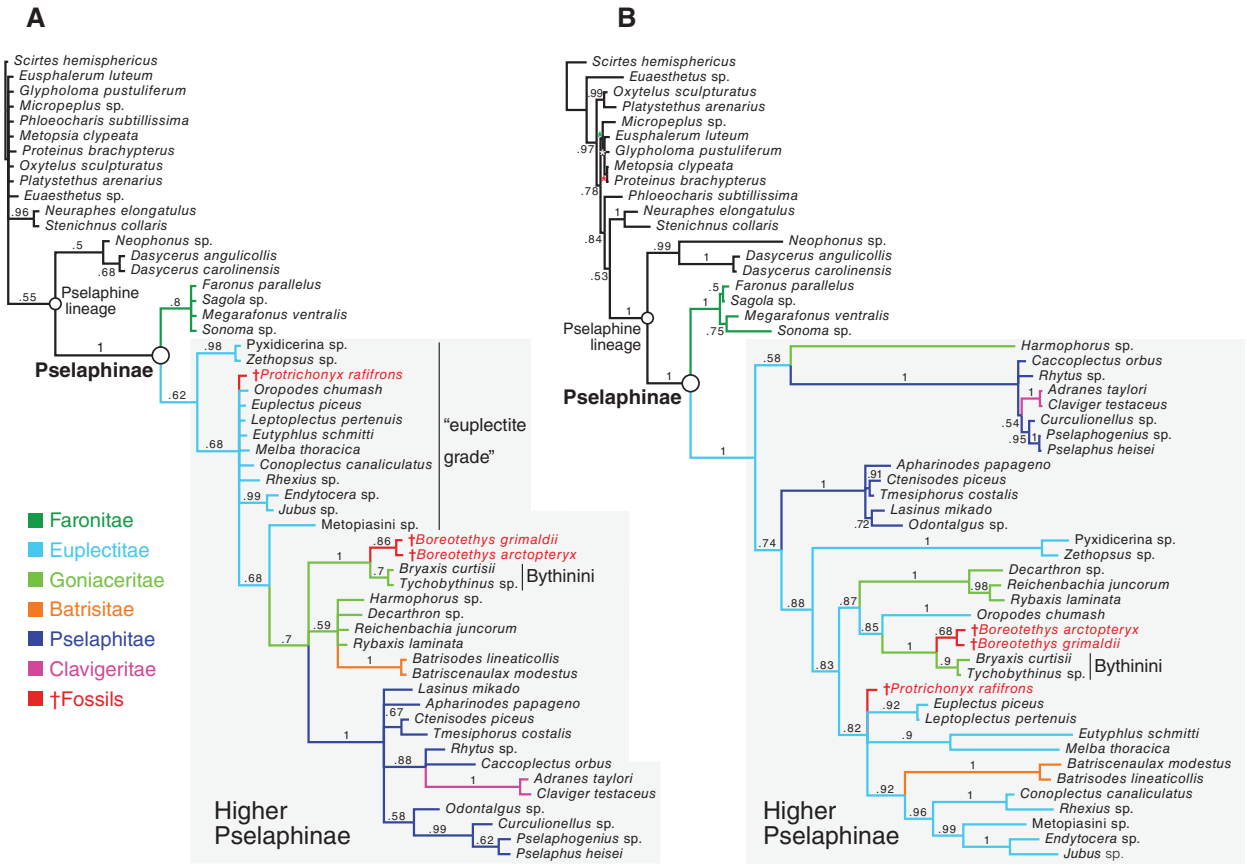

Fig. 6. Phylogenetic placement of new Burmese amber pselaphines. Consensus trees from Bayesian analysis of morphology alone (A) and partitioned analysis of combined morphology and molecular data (B). Values on branches are posterior probabilities (PP). Branches within Pselaphinae are coloured according to supertribe, with the new Cretaceous fossil taxa in red. The higher Pselaphinae clade is boxed in grey. In (A) the 'euplectite grade' is indicated, comprising euplectite taxa (including *Protrichonyx*), which is paraphyletic to the remaining higher Pselaphinae. PP values for asterisked nodes in (B) are 0.61 (black asterisk), 0.78 (white asterisk) and 0.86 (red asterisk).

head shaped into rounded, carinate overhangs covering antennal bases. Basolateral margins of head behind eyes with moderate density of long, thin, erect setae. Gular region anterior to putative gular fovea inflated into mound with short blunt tubercle situated at centre (Fig. 3F); gular mound flanked anteriorly by raised deformations of cuticle with pits that open anteriorly (Fig. 3F; note that these deformations were initially thought to be the maxillary cardines, but appear to be complex gular folds). Eyes with ~25–30 facets, approximately kidney-shaped with shallow ocular canthi (Fig. 3G). Antenna length 0.39 mm. Antennomere 1 elongate-cylindrical and slightly curved mesolaterally, ~3× longer than wide, almost equal in length to antennomeres 3–6 combined (Fig. 3C). Antennomere 2 rounded-cylindrical, 1.4× as wide as long, equal in width to antennomere 1 but half the length. Antennomere 3 rounded-obconical, two thirds as long as antennomere 2 and 0.8× as wide. Antennomeres 4–8 similar in shape and dimension, almost globular between pedicels, equal in width to antennomere 3 and ~0.9× as long. Antennomere 9 transverse-obconical, 1.3× wider and 1.1× longer than antennomere 8. Antennomere 9 quadrate-obconical, 1.5× longer and wider than 8. Antennomere 11 longest, 2× longer than and as broad at base as antennomere 10, broadening to half antennomere length before tapering to rounded apex. Estimated length of extended maxillary palpus 0.22 mm. Palpomere 2 with elongate stem before abruptly broadening to globular apex (Fig. 3G); palpomere 3 short, approximately triangular, orientated with one lateral and two mesal corners; lateral corner rounded. Palpomere 4 flattened (presumed collapsed by compression), elongate, twice as long as wide, with smoothly rounded margins; apical (5th) pseudosegment situated at apex (Fig. 3G).

Thorax: prothorax length 0.20 mm, approximate width at widest point 0.26 mm. Pronotum widening in apical half with smoothly convex, rounded margins to one-third pronotum length; margins in basal two-thirds straight, narrowing to base (Fig. 3A). Edges of pronotum possibly weakly carinate. Basal area of pronotum putatively modified with transverse antebasal impression interrupted by three raised carinae (one medial, two lateral longitudinal) extending from base to almost half pronotum length (this latter apparent modification may have

arisen from damage). Pronotum with sparse, long, erect setae. Paranotal carina extending somewhat dorsally from procoxa to apical margin of prothorax, defining triangular prosternal area (Fig. 3G). Apical margin of prosternum recessed slightly along paranotal carina, so that sides of pronotum extend anteriorly past prosternum in lateral view (Fig. 3G). Prosternum with putative median longitudinal carina. Metaventrite broadly convex (Fig. 3D), but with apparent shallow, median longitudinal declivity.

Abdomen: length along dorsal midline 0.30 mm. Width at widest point (along apical margin of tergite IV) 0.44 mm. Apicolateral corners of paratergites IV–VI angularly projecting (Fig. 3A). Tergites and sternites covered sparsely with raised, posteriorly directed thin, clear setae.

Elytra: elytral length along suture 0.30 mm. Width at widest point 0.44 mm. Elytron with marginal carina extending from humerus to apex. Elytra sparsely covered with regularly spaced, posteriorly directed, long setae, which are more appressed than in other body regions.

Legs: metacoxa barely projecting posteriorly, and with short mesal tubercular projection extending past metatrochanter. Profemora slightly flattened, but femora and tibiae of all legs otherwise slender and lacking modifications. Tarsomeres somewhat tubular, second tarsomeres thicker than third tarsomeres (Fig. 3F). Lengths of leg segments: profemur 0.23 mm, protibia 0.26 mm, protarsus 0.16 mm, mesofemur 0.20 mm, mesotibia 0.26 mm, mesotarsus 0.12 mm, metafemur 0.26 mm, metatibia 0.28 mm, metatarsus 0.16 mm.

Etymology. The species is named in honour of Dr David Grimaldi, curator of fossil insects at AMNH, who has kindly made available amber pselaphines that have significantly enhanced my understanding of the subfamily's evolution.

***Boreotethys arctopteryx* sp.n.**

http://zoobank.org/urn:lsid:zoobank.org:act:1A7FF169-FC87-4E73-BFB1-1C91CBEDBADF

Staphylinoidea: Grimaldi *et al.* (2002): p45, Fig. 29B.

Type material. Holotype (sex unknown, putative male). 'AMBER: MYANMAR (BURMA)/Upper Cretaceous/Kachin: Tanai Village (on Ledo Rd. 105 km NW Myitkyna)/coll. Leeward Capitol Corp., 2000/AMNH Bu-248 // *Pselaphinae* Det. Chatzimanolis 2012.' Specimen in AMNH.

Diagnosis. Boreotethys arctopteryx differs from the type species *B. grimaldii* in that antennomeres 1 and 2 are approximately equal in length and only slightly wider than antennomeres 3–8; the metacoxae project more strongly posteriorly and their separation by the metaventral process is even narrower; the legs, and femora in particular, are thicker; tarsomeres 1 and 2 are approximately equal in width, and the body as a whole is much more densely setose. Possible differences may also exist in vertexal morphology (presence or absence of vertexal foveae) and in the form of the antebasal region of the pronotum.

Description. Body length 0.92 mm (Fig. 4A). Form somewhat flattened. Body dark brown-black, appendages slightly lighter in colouration. Most regions covered in relatively high density of conspicuous, long setae.

Head: length 0.19 mm, width across eyes 0.2 mm (Fig. 4B). Vertexal fovea not apparent. Anterior region of vertex in front of eyes moderately impressed, or collapsed inward due to fossil compression. Dorsolateral edge of head between eye and antennal base carinate. Vertex covered with long setae. Basolateral margins of head behind eyes with thick density of long, erect setae. Gular region obscured by bubbles. Eyes with 40–45 facets (exact number not obvious). Antenna length 0.39 mm. Antennomere 1 elongate-cylindrical, ~2.5× longer than wide, 0.93× as long as antennomeres 3–6 combined (Fig. 4B; note in this image that the antennal scapes are orientated slightly upwards, hence appearing short). Antennomere 2 similar in length to antennomere 1 but slightly narrower. Antennomeres 3–8 similar in width to antennomere 2. Antennomere 3 rounded-obconical, 0.45× as long as antennomere 2. Antennomeres 4–6 similar in shape and dimension, approaching globular, ~0.7× as long as antennomere 3. Antennomere 7 quadrate-obconical, equal in length to antennomere 6. Antennomere 8 transverse-obconical, ~1.2× as wide as long and slightly shorter than antennomere 7. Antennomere 9 transverse-obconical, similar in length but 1.3× as wide as antennomere 8. Antennomere 10 rounded transverse-obconical, 1.5 wider and longer than 9. Antennomere 11 longest, 1.7× the length of antennomere 10 and 1.4× as long as wide, broadening to midpoint before tapering to rounded apex. Mesial face of antennomere 11 weakly concave in apical half. All antennomeres covered with moderate density of long, erect setae, with setal concentration highest around antennomere 11 apex. Estimated length of extended maxillary palpus 0.26 mm. Palpomere 2 elongate, gradually broadening to apex; third palpomere short, approximately triangular, with rounded lateral margin. Palpomere 4 flattened (presumed collapsed by compression), elongate, 2.8 × longer than wide, with straight lateral margin and smoothly rounded mesal margin. Palpomeres 3 and 4 covered in moderate density of long, erect setae (Fig. 4B).

Thorax: prothorax length 0.19 mm, width 0.23 mm. Pronotum broadly convex, with lateral margins rounded, widening to two-fifths pronotum length before narrowing to base. Edges of pronotum not obviously carinate. Basal area of pronotum possibly with median and lateral depressions (likely artefactual). Pronotum relatively densely covered with long, appressed, posteriorly directed setae. Thoracic venter obscured by bubbles.

Abdomen: length along dorsal midline 0.28 mm. Width at widest point (along apical margin of tergite V) 0.33 mm. Basal sulcus-like impressions of tergites V and VI (seen as transverse rows of bubbles across the abdomen in Fig. 4A) may be fossilization artefacts. Tergites and sternites covered in relatively high density of long setae, with apical-most visible sternite (VIII?) uniformly covered with still higher density of shorter setae.

Elytra and flight wings: elytral length along suture 0.26 mm. Combined width at widest point 0.36 mm. Basal half of elytron with two longitudinal impressions, each terminating in putative

basal foveae. Elytron without clear marginal carina, but becoming more sharply margined towards apex. Elytra densely covered with appressed, posteriorly directed, long setae. Full flight wings present (Fig. 4A); lacking veination except in proximate half of anterior quarter; long marginal setae present along posterior edge.

Legs: metacoxae minimally separated by short intercoxal process (Fig. 4C). Legs lacking evidence of modifications. Second tarsomeres barely thicker than third tarsomeres. Dimensions of leg segments: profemur 0.23 mm, protibia 0.23 mm, protarsus 0.12 mm, mesofemur 0.23 mm, mesotibiae obscured, mesotarsus 0.13 mm, metafemur 0.21 mm, metatibia 0.19 mm, metatarsus 0.12 mm.

Etymology. The specific name is a combination of the Greek ἄρκτος (‘arktos’, meaning bear) and πτέρυξ (pteryx, meaning wing), on account of the species’ hairy vestiture, and the fully spread flight wings of the holotype specimen.

Re-evaluation of documented Cretaceous pselaphines

In contrast to Cenozoic fossil Pselaphinae, which are diverse and abundant in Eocene Baltic and Miocene Dominican ambers, the known Cretaceous fossil record of the subfamily is small and poorly studied. Despite the limited material available to date, there are, nevertheless, major ambiguities in published interpretations of these Cretaceous specimens. Re-evaluations of their systematic positions are therefore necessary.

Cretasonoma corinformibus Peris *et al.* (2014), in mid-Cretaceous (Albian) Spanish amber, has external features diagnostic of the Recent supertribe Faronitae, the earliest-diverging clade of Pselaphinae (Newton & Thayer, 1995). A further specimen matching the faronite diagnosis is present in the AMNH Burmese amber collection, but is not described here, and I have seen other, recently mined specimens in Burmese amber that also appear to belong to Faronitae. While modern Faronitae form a defensibly monophyletic group based on both morphology (Newton & Thayer, 1995) and molecular data (Fig. 6; J. Parker, unpublished data; J.S. Park, personal communication), a major caveat applies to the interpretation of fossilized putative Faronitae. The faronite diagnosis is commonly based on easily observable external characters that effectively separate this clade from crown-group higher Pselaphinae: (i) a flattened, parallel-sided body plan, similar to the generalized rove beetle form; (ii) simple antennae lacking an apical club (Fig. 7A); (iii) tarsi, though reduced to three segments as in other pselaphines, comprising short first and second tarsomeres and bearing two tarsal claws of equal size (Fig. 7D), as in the sister subfamilies Protopselaphinae, Dasycerinae and Neophoninae, which together form the ‘pselaphine lineage’ of omaliine group Staphylinidae (Newton & Thayer, 1995); (iv) short trochanters on all legs; (v) contiguous, posteriorly projecting metacoxae (Fig. 7C); (vi) the highest number of foveae decorating the body in a hypothetical pselaphine groundplan pselaphine pattern (sensu Chandler, 2001), including on the elytral disc (Fig. 7B). All such characters are, however, considered plesiomorphic in Pselaphinae (Newton & Thayer, 1995; Chandler, 2001), and in fact true morphological autapomorphies of Faronitae require dissection to observe. The asymmetric faronite aedeagus, which lacks an obvious median lobe, dorsal diaphragm or internal musculature, is seemingly unique among pselaphines and allied staphylinid subfamilies of the omaliine group (Chandler, 2001). Genitalic structure is challenging or impossible to assess in fossilized specimens. Consequently, the aforementioned external characters simply serve to place a specimen outside of the higher Pselaphinae. On their own, they cannot be used to determine whether a specimen truly belongs within crown-group Faronitae, as opposed to the stem group of all Pselaphinae, the stem-group of Faronitae, or the stem-group of the higher Pselaphinae. However, while this caveat applies to the interpretation of *Cretasonoma*, I cannot provide observational counterevidence from the specimens to conclude that the genus is definitively not a crown-group faronite. *Cretasonoma* is therefore left in Faronitae.

Further issues surround two other published Cretaceous specimens. Both may superficially be perceived as crown-group higher pselaphines, but each appears to have been erroneously interpreted, and their placements are reassessed here. *Penarhytus tenebris* Peris, Chatzimanolis and Delclòs in mid-Cretaceous (Albian) Spanish amber was tentatively placed within Arhytodini (Peris *et al.*, 2014), a tribe of the higher Pselaphinae. Monophyly of Arhytodini is questionable due to a lack of clear autapomorphies to separate them from several other pselaphine tribes, but arhytodines are nevertheless extremely distinguishable from other pselaphines, with distinctive and apparently specialized morphologies. Depending on the genus, arhytodines show a varying combination of derived characters: (i) sponge-like (squamous) pubescence commonly filling characteristic sulci and foveae on various parts of the body; (ii) strongly modified antennae, which can be geniculate, moniliform, exaggerated in length, show atypical patterns of antennomere sizes, as well as fusions of antennomeres; (iii) enlarged eyes; (iv) a pronounced frontal rostrum; (v) reduced maxillary palpi that are small and/or have a reduced number of palpomeres; (vi) spines along the length of tibiae and femora; (vii) modified tarsomeres of varying relative sizes; (viii), single tarsal claws; (ix) elongate mesotrochanters; (x) distant metacoxae.

I have examined the holotype of *P. tenebris* and it does not possess any such character states that would justify a placement in Arhytodini. *Penarhytus* exhibits a generalized and primitive pselaphine morphology, with important characters leading to a placement outside of the higher Pselaphinae: (i) two tarsal claws; (ii) short second tarsomeres; (iii) metacoxae near-contiguous and apparently projecting posteriorly; (iv) importantly, the mesotrochanters of *Penarhytus*, mentioned in the discussion (but not explicitly in the description, nor depicted in the illustration) as being elongate (a derived condition seen in certain tribes of higher Pselaphinae, including Arhytodini) cannot be viewed with sufficient clarity to judge their form. Based on its observable characters, *Penarhytus* approaches the faronite diagnosis outlined earlier. Differences exist in its trunk shape, which is

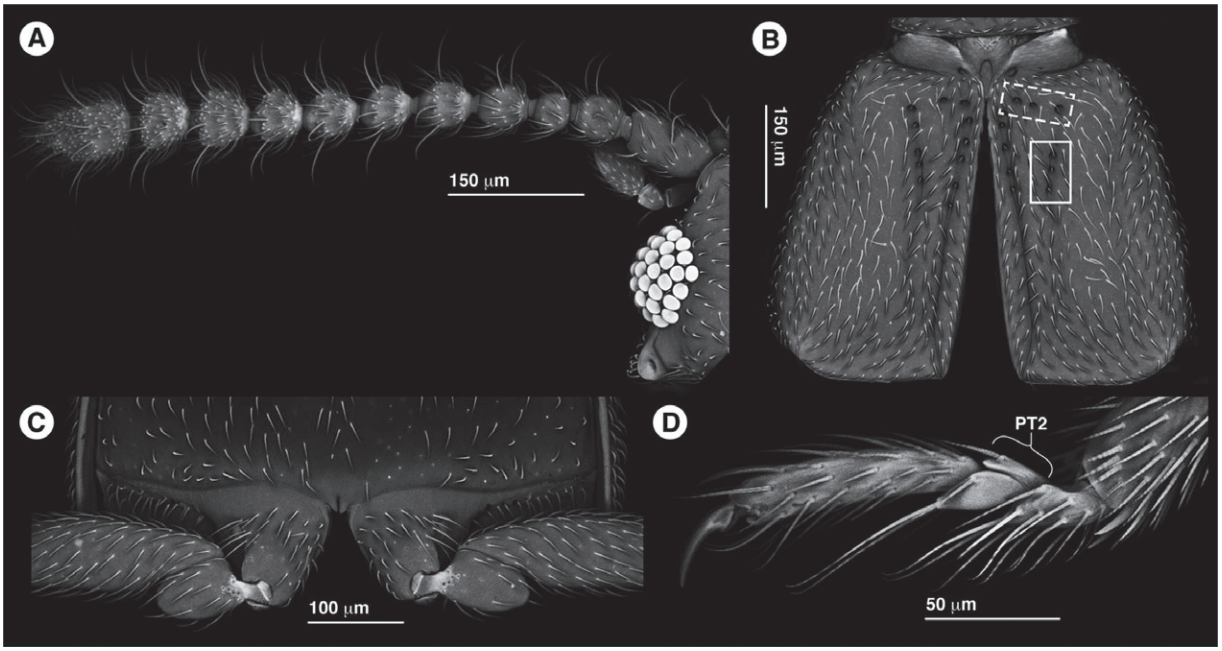

Fig. 7. Morphology of Recent Faronitae. Confocal reconstructions of *Faronus parallelus* (Bulgaria). (A) Left antenna, showing lack of apical club. (B) Elytra, showing foveae on disc (e.g. in box with solid line) as well as base (dashed box). (C) Near-contiguous, conically projecting metacoxae, separated by minimal intercoxal process. (D) Protarsus with short tarsomere 2; note that two equally sized tarsal claws are present but only one is visible in this image.

broader than is typical in Faronitae, and its antennae, which are somewhat more clubbed, although some Recent faronite genera, such as *Pseudostenosagola* Park and Carlton, have equivalently clubbed antennae (Park & Carlton, 2014). The most significant difference is that *Penarhytus* has slightly unequally sized tarsal claws, a character state not mentioned in the original description, and a genuine departure from the faronite diagnosis. Unequally sized tarsal claws are a derived state in Pselaphinae, implying that although *Penarhytus* does not belong within crown-group higher Pselaphinae, it shares one unambiguous, derived state with this clade, and could well be a stem-group. However, pending a phylogenetic assessment of this stem hypothesis, *Penarhytus* is here removed from Arhytodini and simply placed *incertae sedis* in Pselaphinae, outside of higher Pselaphinae.

A bigger palaeontological puzzle is presented by an undescribed compression from the Early Cretaceous (Aptian) Koonwarra fossil bed, Australia, and ascribed to Pselaphinae by Jell and Duncan (Jell & Duncan, 1986; Jell, 2006). The specimen, P103321 of the Museum Victoria collection, does indeed look like a pselaphine in Jell and Duncan's original photograph, and the authors interpret the fossil as: (i) representing the dorsal surface of a specimen; (ii) possessing shortened elytra; (iii) exposed abdominal tergites visible; and (iv) a swollen profemur covering a small head (Fig. 8A). Such an interpretation agrees with a generalized Pselaphinae body plan, and would make P103321 the oldest-known pselaphine fossil; moreover, given its compact, globular form, a plausible higher pselaphine. I obtained new, high-resolution colour photographs of part and counterpart of P103321 (Figs 8A, B), which revealed putative characters that were not evident in the original photograph. Based on the new images, I offer an alternative interpretation of the compression that raises doubts over its proposed taxonomic affinity. The original and new interpretations are depicted in Fig. 8C, D. Central to the reinterpretation was the realization that the entire right and left mesofemora may both be visible (Fig. 8D). It follows that the *right ventrolateral face* of a beetle is, in fact, in view. Proximal leg structures – including putative coxae – may indeed be visible, attaching the femora to the underside of the body. The region previously interpreted as short elytra can readily be reinterpreted as meso-metaventrite, and what were previously exposed tergites may in fact be sternites (Fig. 8D).

This ventralized reinterpretation, further elaborated in the Fig. 8 legend, leaves no features to strongly link P103321 to Pselaphinae. A number of beetle families match this configuration and overall shape in ventrolateral view, and the conclusion as to which one fits best is open to speculation. If, indeed, the head is visible, and acutely triangular with strong occipital constriction as in Fig. 8D, then Anthicidae or Aderidae could be contenders (if the specimen is in ventrolateral view, then the elytra are necessarily obscured by the body and there is no reason to believe they are short – in fact, long elytra might be indicated by the continuous, unbroken dorsal edge of the fossil posterior to the pronotum, especially evident in counterpart B in Fig. 8B). It should also be noted that although the antennae are not complete, the thick antennomeres and absence of an obvious club are again not particularly pselaphine-like (aside from Faronitae which do match the shape of P103321, and a few specialized inquilinous genera); likewise, the clavate

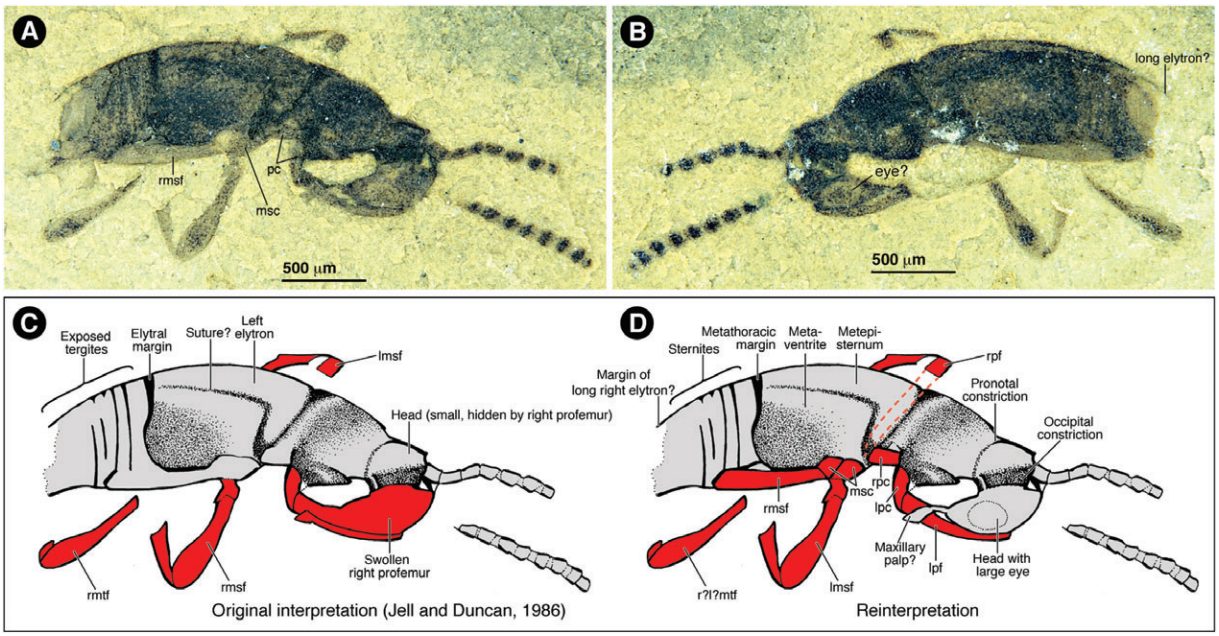

Fig. 8. Alternative interpretations of an Early Cretaceous putative pselaphine compression. (A, B) Part and counterpart of Museum Victoria specimen P103321 from the Koonwarra fossil bed, with reinterpreted putative structures indicated: msc, mesocoxae; pc, procoxae; rmsf, right mesofemur. (C, D) Diagrams of alternative interpretations, with legs highlighted in red. The following interpretations are mostly based on the fossil part in (A). (C) Original interpretation (Jell & Duncan, 1986; Jell, 2006). The dorsal side of a beetle is perceived, with short elytra exposing a segmented abdomen. The observable faces of the legs are inferred to be lateral (r/lmsf, right/left mesofemur; rmtf, right metafemur). An enlarged profemur covers a seemingly tiny head. (D) Reinterpretation. The right mesofemur (rmsf) appears to be observable, indicating that the ventrolateral side of a beetle is, in fact, in view. The short elytra are reinterpreted as meso-metaventrite, and the tergites as sternites (the elytra may, in fact, be full length, as indicated by the uninterrupted dorsal margin of the body posterior to the pronotum, most evident in counterpart B). The faces of the legs are inferred to be mesial and proximal leg characters (coxae) might now be discernible (the reorientation demands the left and right legs swap relative to the former interpretation); r/lpf, right/left profemur; r/lpc, right/left procoxa. The orange dashed line indicates the inferred position of the right profemur, lying across the body. Whether it is the right or left metafemur that is visible is now equivocal (hence labelled 'r?l?mtf'). A large circular eye may be visible on a normally sized head, which is orientated to point posteriorly under the beetle (putative left maxillary palpomere is indicated). There are distinct pronotal and occipital constrictions. Note that the top antenna may be coiled around at the base, appearing to emerge from the pronotum.

femora are more akin to those of Scydmaeninae (Staphylinidae) and some Anthicidae. Regardless of the true identity of P103321, radically different interpretations of this fossil are evidently possible. Ambiguity hangs over what kind of beetle P103321 really is, and its assignment to Pselaphinae is questionable.

In summary, all Cretaceous pselaphines described or explicitly documented in the literature prior to the current study belong outside of the higher Pselaphinae or do not represent definitive pselaphines.

Discussion

Origin and diversification of higher Pselaphinae

The higher Pselaphinae arguably ranks among the most poorly studied of animal clades, but the number of described species nevertheless rivals that of the entire class Aves. The fossils described in this study begin to clarify the timescale over which this exceptional cladogenesis has occurred. The close phylogenetic relationship of the new taxa, *Protrichonyx* and *Boreotethys*, to certain modern clades within the higher Pselaphinae (Fig. 6) provides direct evidence that higher pselaphines had commenced diversification by at least the mid-Cretaceous. Still more significantly, the evolutionary origin of the higher Pselaphinae as a whole may be put back substantially further in time, by considering the Laurasian palaeolocality of these specimens in the context of the higher Pselaphinae's modern, largely Gondwanan zoogeographic distribution.

Pselaphines typically show high endemism at both genus and species levels, presumably due to their dispersal being limited by small body size and narrow niche preferences (Reichle, 1966, 1967). If we consider the present-day geographic ranges of pselaphine taxa, this could therefore help to pinpoint ancestral origins (Carlton, 1990; Carlton & Cox, 1990). The global distributions of Recent pselaphine tribes are summarized in Table 2, and reveal what appears to be a pervasive Gondwanan bias. Two-thirds of all Pselaphine tribes are either confined to or have their largest fractions of genera endemic to regions that are derived from Gondwana (Table 2, top sector). The inference is that these regions of high endemicity probably represent the tribes' zoogeographic cradles (Jeannel, 1950b; Hlaváč

Table 2. Zoogeography of Recent Pselaphinae. Tribes are listed with their contemporary distributions. The table is split into a top sector (tribes with putative origin on Gondwana or one of its descendent landmasses), middle sector (tribes with putative origin on Laurasia or descendent landmasses) and bottom sector (tribes/supertribes with putative Pangaean or unknown origin). Asterisks denote tribes of doubtful monophyly. Tribes in bold contain myrmecophiles.

Tribe	Present-day zoogeographic range
Arhytodini	Afrotropics, Australasia, Indomalaya, Neotropics (only *Caccoplectus* reaches southern US)[a]
Attapseniini	Neotropics[b]
Barroselini	Afrotropics
Brachyglutini*	Global (generic bias throughout Gondwanan regions)[c]
Bythinoplectini	Afrotropics, Australasia, Indomalaya, Neotropics (of 71 genera, two reach southern US and two Japan)
Clavigerini	Global (but absent from New Zealand, Southern South America, genus-poor in New World)[d]
Colilodionini	Indomalaya[d]
Ctenistini	Global (generic bias throughout Gondwanan regions)
Cyathigerini	Afrotropics, Australia, Indomalaya (one genus reaching Japan)
Dimerini	Afrotropics, Australasia, Neotropics, Indomalaya, Japan
Goniacerini	Afrotropics, Neotropics
Hybocephalini	Afrotropics, Australia, Indomalaya
Iniocyphini*	Afrotropics, Australasia, Neotropics, Indomalaya, Japan
Jubini	Neotropics
Machadoini	Afrotropics
Metopiasini	Neotropics
Odontalgini	Afrotropics, Australia, Indomalaya (one genus reaching Japan)
Pachygastrodini	Afrotropics
Phalepsini	Neotropics
Proterini*	Pantropical
Pselaphini	Global (generic bias throughout Gondwanan regions)
Tiracerini	Australasia[d]
Tmesiphorini	Afrotropical, Australia, Indomalaya, Nearctic (one genus reaching Japan)[e]
Tyrini*	Global (generic bias throughout Gondwanan regions)[f]
Amauropini	Eastern Nearctic, western Palearctic[g]
Arnyliini	Indomalaya
Batrisini*	Global (but absent from New Zealand)[h]
Bythinini	Holarctic
Imirini	Western Palearctic (southern Europe)
Pygoxyini	Western Palearctic (southern Europe)
Speleobamini	Nearctic
Thaumastocephalini	Western Palearctic
Tychini	Holarctic
Valdini	Nearctic
Faronitae	Global (temperate)
Euplectini	Global
Mayetiini	Afrotropics, Nearctic, Neotropics, Palearctic,
Trichonychini*	Global
Trogastrini	Australia, Europe, Nearctic, Neotropics, New Zealand

[a]Recent or fossil arhytodines are now known from tropical areas throughout Gondwanan-descendent landmasses (Löbl, 2000; Chandler, 2001; Parker & Grimaldi, 2014).

[b]Monogeneric tribe, obligate symbiont of *Atta* leafcutter ant colonies, perhaps derived from Neotropical Tyrini.

[c]Two exclusively Neotropical subtribes of Brachyglutini, Eupseniina and Baradina do not belong within this tribe (J. Parker, unpublished).

[d]Collectively, Clavigerini, Colilodionini and Tiracerini form the supertribe Clavigeritae, a large clade of obligate myrmecophiles. A Late Cretaceous/Early Palaeocene origin in Indomalayan or Australasian region was inferred from molecular dating by Parker & Grimaldi (2014).

[e]Tmesiphorini is almost exclusively Old World; only some species of *Tmesiphorus* occur in the Nearctic, possibly Beringian dispersal of this otherwise East Asian/Australian genus.

[f]Jeannel inferred a Gondwanan origin of Tyrini (Jeannel, 1950b), a conclusion supported by analysis of the distribution of genera and species (Hlaváč & Chandler, 2005).

[g]Cavernicolous troglomorphs, probably derived from within tropically dominant Batrisini, but have a range that spans the Appalachian-Hercynian orogeny.

[h]Batrisini are strongly diversified at genus level in Afrotropical and Indomalayan regions, but are genus-poor in the Neotropics. They are also somewhat diversified in the Holarctic, absent from New Zealand, and probably paraphyletic with respect to the Amauropini, a Holarctic group that are demonstrably Laurasian (see the above footnote *g*). A Laurasian origin is thus tentatively suspected, with dispersal into many Gondwana-derived regions.

& Chandler, 2005). In contrast, a handful of tribes are exclusively Laurasian (Table 2, middle sector), and the discovery of higher Pselaphinae in Burmese amber – including *Boreotethys*, a stem-group of Recent, Holarctic Bythinini – confirms that higher Pselaphinae inhabited Laurasia long before its suturing with Gondwanan landmasses in the Cenozoic.

Thus, evidence exists of an ancient presence of largely mutually exclusive subsets of higher pselaphine lineages on Gondwana and Laurasia. The higher Pselaphinae as a whole might therefore have originated when the supercontinents were united in the Jurassic. The fact that the Recent higher Pselaphinae are not split into reciprocally monophyletic Laurasian and Gondwanan clades, (J. Parker, unpublished data, also evident in Fig. 6) indicates further that some degree of basal cladogenesis had already occurred in higher pselaphines prior to Pangaean rifting. Congruent with a Pangaean origin of the higher Pselaphinae is the observation that the clade's coeval sister group – the supertribe Faronitae – has a widely disjunct distribution, inhabiting temperate regions of the northern and southern hemispheres, and is largely absent from the tropics except for some cooler, high elevation sites (Chandler, 2001). Jeannel believed Faronitae were a Gondwanan group that dispersed to the northern hemisphere (Jeannel, 1961), but given the newly hypothesized Jurassic age of the Faronitae–higher Pselaphinae split, it is conceivable that Faronitae's modern range may have arisen vicariantly, following the break-up of Pangaea.

Hard evidence for this evolutionary scenario rests on the congruence of future Cretaceous pselaphine discoveries with the Laurasian–Gondwanan tribal segregation of the higher Pselaphinae, and on confirming the reality of Jurassic higher pselaphines. Jurassic fossils of multiple other staphylinid subfamilies have now been recovered, including Oxytelinae and Piestinae (Tikhomirova, 1968), Glypholomatinae (Cai *et al.*, 2012), Olisthaerinae (Ryvkin, 1985; Cai *et al.*, 2014), Omaliinae (Tikhomirova, 1968; Ryvkin, 1985; Cai & Huang, 2013) and Tachyporinae (Tikhomirova, 1968; Cai *et al.*, 2013). Likely Jurassic origins of Staphylininae and Paederinae have been inferred on the basis of their considerable diversification by the Early Cretaceous (Solodovnikov *et al.*, 2013), while support for a Jurassic origin of Solieriinae, a subfamily with a single Recent genus from southern South America, comes from the discovery of mid-Cretaceous solieriines in Lebanese and Burmese amber (Thayer *et al.*, 2012). The Jurassic has thus been proposed as major period of diversification of Staphylinidae into modern subfamilies (Chatzimanolis *et al.*, 2012; Grebennikov & Newton, 2012). Pselaphinae are evidently also contenders for having originated at some time during this period, with important early divergences having potentially occurred in this subfamily by the end of the Jurassic.

Such an age has ramifications for subfamilies allied to Pselaphinae in the 'omaliine group' of Staphylinidae. Support for this clade has come from cladistic analysis of morphology (Newton & Thayer, 1995), whereas the limited number of molecular studies thus far have yielded support for only part of it. The present study, as well as a recent phylogenetic analysis of staphyliniform relationships (McKenna *et al.*, 2014), provides molecular evidence for the 'pselaphine lineage' comprising Pselaphinae + Dasycerinae + Neophoninae (and presumably also the elusive Protopselaphinae, which thus far lack any molecular data). Although both of these molecular studies used limited gene sampling (one and two gene regions, respectively), the congruence of at least this part of the omaliine group with morphology implies that the pselaphine lineage is a real clade. Aside from Pselaphinae, the only other subfamily of the pselaphine lineage with published fossils is Dasycerinae, with the genus *Protodasycerus* recently described from Burmese amber (Yamamoto, 2016). I posit that all four subfamilies may extend back to the Jurassic.

Substantial pselaphine diversification probably happened during the Cretaceous, and crown-groups of most Recent tribes appear to have arisen by the Eocene at the latest (Fig. 1). At present, the only explicit dating analysis in Pselaphinae is that of Parker & Grimaldi (2014), who described a stem-group of the supertribe Clavigeritae in Early Eocene Cambay amber, and molecularly dated the origins of clavigerite tribes to a window approximately spanning the K–Pg boundary. Further support for considerable tribal-level diversity having arisen by the Eocene comes from the principal work on Lutetian Baltic amber pselaphines by Schaufuss (1890). His two dozen descriptions are superficial, and the material is now seemingly lost, perhaps having been destroyed in World War II (A.F. Newton and D.S. Chandler, personal communication), yet almost all specimens appear to have belonged to Recent tribes (Fig. 1) and most were placed into modern genera (Newton & Chandler, 1989). Morphologically modern and diverse Pselaphinae also seem to have become relatively ecologically abundant by the Middle Eocene, as suggested by their frequency relative to other beetle groups in Baltic amber (e.g. Kulicka & Ślipiński, 1996). This high diversity and abundance are sustained in younger, Miocene/Oligocene Dominican and Mexican ambers, which hold an exceptionally rich but completely unstudied pselaphine fauna, with many Recent Neotropical genera, and examples of possible Recent species (Chandler & Wolda, 1986). With the construction of a reliable pselaphine phylogeny, hypotheses regarding the diversification and historical biogeography of this subfamily will no doubt become more finely resolved.

A morphological predisposition to inquilinism?

The inferred antiquity of the higher Pselaphinae also provides insights into a pervasive aspect of pselaphine biology: the symbioses of many taxa with ants (myrmecophily). Such inquilinous species are known from most tribes of higher Pselaphinae (indicated in Table 2) (Park, 1942; Kistner, 1982; Parker & Grimaldi, 2014; Parker, 2016), with the clade showing an evolutionary predisposition to this lifestyle rivalled in other Staphylinidae only by the Aleocharinae. The preponderance of higher pselaphines in heavily ant-dominated tropical forest floors – a habitat in which many other arthropod groups appear to fare poorly (Wilson, 1990; Wilson & Hölldobler, 2005) – implies a general adeptness for ecological coexistence with ants. In contrast, myrmecophilous species are not known in Faronitae, the earliest diverging lineage of Pselaphinae (Newton & Thayer, 1995)

(Fig. 6), and members of this group are largely excluded from tropical litter, aside from high elevation localities where ants are scarce.

Burmese amber and near-contemporaneous mid-Cretaceous deposits harbour the oldest-known definitive ants (Grimaldi & Agosti, 2000; Wilson & Hölldobler, 2005; LaPolla & Dlussky, 2013), and molecular dating suggests that ants did not originate substantially before this time, most probably during the Early Cretaceous (Brady *et al.*, 2006; Moreau & Bell, 2013). Although neither *Boreotethys* nor *Protrichonyx* show any specializations for inquilinism, they nevertheless reveal that the higher Pselaphine, a clade seemingly preadapted for myrmecophily, is equal in age to the earliest ants, and given its newly hypothesized Jurassic origin, potentially far older. Most mid-Cretaceous ants belong to the extinct formicid stem-group Sphecomyrminae (Grimaldi *et al.*, 1997; Engel & Grimaldi, 2005; Barden & Grimaldi, 2014), although a handful of exceptional crown-group ants have been recovered (Grimaldi & Agosti, 2000; Nel *et al.*, 2004). Cumulatively, however, Cretaceous ants are rare, comprising less than 1% of the total insect fossils in any given deposit, and it was not until the Cenozoic that ants – much like pselaphines – became diverse, abundant and definitively modern in form (Grimaldi & Agosti, 2000; Wilson & Hölldobler, 2005; LaPolla & Dlussky, 2013; Barden & Grimaldi, 2014; Ward, 2014). The earliest known morphologically specialized myrmecophile of any group of arthropods is *Protoclaviger trichodens* Parker and Grimaldi – a higher pselaphine dating to the Early Eocene – and it may be that the Late Cretaceous/Early Cenozoic marked a time when both pselaphines and ants rose to prominence and myrmecophilous links were first forged.

Traits that contribute to the higher pselaphine predisposition to myrmecophily are unclear, but their diminutive size and novel, consolidated body plan may play a role. If pselaphines derive from within Staphylinidae, as both morphological and molecular phylogenies suggest (Newton & Thayer, 1995; McKenna *et al.*, 2014), then evolution of their external morphology must have followed a scenario in which the flexible, flattened and elongate body plan of staphylinid ancestors became more compact and rigid. Structural modifications that appear instrumental include a thickening of the cuticle, shortening or loss of intersegmental membranes, and the appearance of foveae, sulci and associated endoskeletal struts and apodemes that provide internal bracing (Ohishi, 1986; Chandler, 2001). In most groups of higher Pselaphinae, the body shape has undergone further modifications such that the abdomen is shorter, broader and dorsoventrally less flattened, creating the familiar compact form. Relative to other staphylinids that rapidly hunt down their quarry, pselaphines move slowly, stalking prey items and seizing them in their mandibles, or employing raptorial legs or elaborate maxillary palpi to trap them (Schomann *et al.*, 2008). Evolution of this mode of prey capture may have driven the exchange of body flexibility for consolidated rigidity. Pselaphines are very small beetles (even compared with most staphylinids), and the strengthened pselaphine integument may be beneficial for withstanding compression while moving through substrata. More importantly perhaps, it provides a degree of physical protection from larger-bodied predators (Newton & Thayer, 1995). The compact body shape of most higher Pselaphinae enables retraction of the head and appendages to form a protective ball (conglobation) – a stance that at least some species assume during aggressive encounters with ants (effectiveness of the heavy integument and conglobation in evading ant aggression is shown in Video S1).

Faronitae retain an elongate and parallel-sided body, with abdominal segments that are relatively more flexible and articulate more than in most higher pselaphines. They also lack any kind of abdominal defensive exocrine gland (Newton & Thayer, 1995), a common deterrent mechanism seen in many other staphylinid groups with flexible abdomens (Dettner, 1993). Faronites may therefore be correspondingly less well protected in encounters with ants. Hence, the small size and protective morphology of higher pselaphines may have primed these beetles to withstand the rising ecological pressure from ants during the Cenozoic, perhaps accounting for the contemporary diversity and abundance of higher Pselaphinae in ant-rich tropical litter (Parker, 2016), where they might be the predominant beetle taxon (Olson, 1994; Sakchoowong *et al.*, 2007). The unique morphology of higher pselaphines may then have secondarily permitted colony intrusion, where, as predators, they could target the ant brood (and other nest microarthropods). Such an intrinsic capacity to engage in facultative associations with ants may explain the recurrent evolution of obligate myrmecophily across the higher Pselaphinae.

Supporting Information

Additional Supporting Information may be found in the online version of this article under the DOI reference: 10.1111/syen.12173

Figure S1. Supporting analyses for the phylogenetic placement of new Burmese amber pselaphines. (A) Bayesian consensus tree from analysis of molecular data alone. Values on branches are posterior probabilities (PP). Branches within Pselaphinae are coloured according to supertribe and the higher Pselaphinae is boxed in grey. (B–D) Bootstrap consensus trees from parsimony analyses of the molecular data alone (B), morphological data alone (C), and combined data (D). Values on branches are bootstrap percentages >50 from 1000 replicates. The higher Pselaphinae is boxed in grey, and fossil taxa are in red.

Table S1. Taxon inventory for phylogenetic analysis, with Genbank accession IDs.

File S1. MrBayes Nexus file for Bayesian combined analysis of morphological and molecular data.

Video S1. Two *Plagiophorus* (Pselaphinae: Cyathigerini) beetles attacked by the ant *Pachycondyla javana*. The heavy integument, combined with retraction of the appendages, protects the pselaphines from damage inflicted by the ant's large mandibles. Specimens from Okinawa, Japan.

Acknowledgements

I thank David Grimaldi (AMNH) for preparing and making available the amber pselaphines described in this study, David Peris (Universitat de Barcelona) for providing the *Penarhytus* holotype for my observation, and David Holloway (Museum Victoria, Melbourne) and Peter Jell (University of Queensland) for, respectively, producing new images of the Koonwarra compression fossil, and literature and discussion relating to this specimen. Alfred Newton (Field Museum, Chicago) kindly accessed his database to give an up-to-date figure of the exact number of described species of Pselaphinae. I am grateful to Rostislav Bekchiev, Chris Carlton, Michael Caterino, Donald Chandler, Darren Mann, Alfred Newton Shuhei Nomura and Margaret Thayer for contributing specimens. Chris Carlton (Louisiana State University), Taro Eldredge (Univ. Kansas) and David Grimaldi provided important comments on the manuscript.

References

Akre, R.D. & Hill, W.B. (1973) Behavior of *Adranes taylori*, a myrmecophilous beetle associated with *Lasius sitkaensis* in the Pacific Northwest (Coleoptera: Pselaphidae; Hymenoptera: Formicidae). *Journal of the Kansas Entomological Society*, **46**, 526–536.

Barden, P. & Grimaldi, D. (2014) A diverse ant fauna from the mid-Cretaceous of Myanmar (Hymenoptera: Formicidae). *PLoS ONE*, **9**, e93627.

Brady, S.G., Schultz, T.R., Fisher, B.L. & Ward, P.S. (2006) Evaluating alternative hypotheses for the early evolution and diversification of ants. *Proceedings of the National Academy of Sciences of the United States of America*, **103**, 18172–18177.

Cai, C.-Y. & Huang, D.-Y. (2013) Sinanthobium daohugouense, a tiny new omaliine rove beetle (Coleoptera: Staphylinidae) from the Middle Jurassic of China. *The Canadian Entomologist*, **145**, 496–500.

Cai, C., Huang, D., Thayer, M.K. & Newton, A.F. (2012) Glypholomatine rove beetles (Coleoptera: Staphylinidae): a Southern Hemisphere Recent group recorded from the Middle Jurassic of China. *Journal of the Kansas Entomological Society*, **85**, 239–244.

Cai, C.-Y., Yan, E.V., Beattie, R., Wang, B. & Huang, D.-Y. (2013) First rove beetles from the Jurassic Talbragar Fish Bed of Australia (Coleoptera, Staphylinidae). *Journal of Paleontology*, **87**, 650–656.

Cai, C., Beattie, R. & Huang, D. (2014) Jurassic olisthaerine rove beetles (Coleoptera: Staphylinidae): 165 million years of morphological and probably behavioral stasis. *Gondwana Research*, **28**, 1579–1584.

Cammaerts, R. (1974) Le systeme glandulaire tegumentaire du coleoptere myrmecophile *Claviger testaceus* Preyssler, 1790 (Pselaphidae). *Zeitschrift für Morphologie der Tiere*, **77**, 187–219.

Cammaerts, R. (1992) Stimuli inducing the regurgitation of the workers of *Lasius flavus* (Formicidae) upon the myrmecophilous beetle *Claviger testaceus* (Pselaphidae). *Behavioural Processes*, **28**, 81–96.

Carlton, C.E. (1990) Biogeographic affinities of pselaphid beetles of the eastern United States. *The Florida Entomologist*, **73**, 570–579.

Carlton, C.E. & Cox, R.T. (1990) A new species of *Arianops* from central Arkansas and biogeographic implications of the interior highlands *Arianops* species (Coleoptera: Pselaphidae). *The Coleopterists Bulletin*, **44**, 365–371.

Chandler, D.S. (1990) Insecta: Coleoptera Pselaphidae. *Soil Biology Guide* (ed. by D.L. Dindal), pp. 1175–1190. John Wiley and Sons, New York, New York.

Chandler, D.S. (2001) *Biology, Morphology and Systematics of the Ant-Like Litter Beetles of Australia (Coleoptera: Staphylinidae: Pselaphinae)*, Vol. 15. Associated Publishers, Gainesville, Florida.

Chandler, D.S. & Wolda, H. (1986) Seasonality and diversity of *Caccoplectus*, with a review of the genus and description of a new genus, *Caccoplectinus* (Coleoptera: Pselaphidae). *Zoologische Jahrbücher, Abteilung für Systematik, Ökologie und Geographie der Tiere*, **113**, 469–524.

Chatzimanolis, S., Grimaldi, D.A., Engel, M.S. & Fraser, N.C. (2012) *Leehermania prorova*, the earliest staphyliniform beetle, from the late Triassic of Virginia (Coleoptera: Staphylinidae). *American Museum Novitates*, **3761**, 1–28.

Coulon, G. (1989) Révision générique des Bythinoplectini Schaufuss, 1890 (=Pyxidicerini Raffray, 1903, syn. nov.) (Coleoptera, Pselaphidae, Faroninae). *Mémoires de la Société Royale Belge d'Entomologie*, **34**, 1–282.

Darriba, D., Taboada, G.L., Doallo, R. & Posada, D. (2012) jModelTest 2: more models, new heuristics and parallel computing. *Nature Methods*, **9**, 772.

Dettner, K. (1993) Defensive secretions and exocrine glands in free-living staphylinid beetles – their bearing on phylogeny (Coleoptera: Staphylinidae). *Biochemical Systematics and Ecology*, **21**, 143–162.

Donisthorpe, H. (1927) *The Guests of British Ants: Their Habits and Life Histories*. George Routledge & Sons, London.

Dutta, S., Mallick, M., Kumar, K., Mann, U. & Greenwood, P.F. (2011) Terpenoid composition and botanical affinity of Cretaceous resins from India and Myanmar. *International Journal of Coal Geology*, **85**, 49–55.

Engel, M.S. & Grimaldi, D.A. (2005) Primitive new ants in Cretaceous Amber from Myanmar, New Jersey, and Canada (Hymenoptera: Formicidae). *American Museum Novitates*, **3485**, 1–24.

Felsenstein, J. (1985) Confidence-limits on phylogenies–an approach using the bootstrap. *Evolution*, **39**, 783–791.

Gilbert, M.T.P., Moore, W., Melchior, L. & Worobey, M. (2007) DNA extraction from dry museum beetles without conferring external morphological damage. *PLoS ONE*, **2**, e272.

Goloboff, P.A., Farris, J.S. & Nixon, K.C. (2008) TNT, a free program for phylogenetic analysis–Goloboff–2008 - Cladistics–Wiley online library. *Cladistics*, **24**, 774–786.

Grebennikov, V.V. & Newton, A.F. (2009) Good-bye Scydmaenidae, or why the ant-like stone beetles should become megadiverse Staphylinidae sensu latissimo (Coleoptera). *European Journal of Entomology*, **106**, 275–301.

Grebennikov, V.V. & Newton, A.F. (2012) Detecting the basal dichotomies in the monophylum of carrion and rove beetles (Insecta: Coleoptera: Silphidae and Staphylinidae) with emphasis on the Oxyteline group of subfamilies. *Arthropod Systematics & Phylogeny*, **70**, 133–165.

Grimaldi, D. & Agosti, D. (2000) A formicine in New Jersey Cretaceous amber (Hymenoptera: Formicidae) and early evolution of the ants. *Proceedings of the National Academy of Sciences of the United States of America*, **97**, 13678–13683.

Grimaldi, D., Agosti, D. & Carpenter, J.M. (1997) New and rediscovered primitive ants (Hymenoptera: Formicidae) in Cretaceous amber from New Jersey, and their phylogenetic relationships. *American Museum Novitates*, **3208**, 1–43.

Grimaldi, D.A., Engel, M.S. & Nascimbene, P.C. (2002) Fossiliferous Cretaceous amber from Myanmar (Burma): its rediscovery, biotic diversity, and paleontological significance. *American Museum Novitates*, **3361**, 1–71.

Hammond, P.M. (1979) Wing-folding mechanisms of beetles, with special reference to investigations of adephagan phylogeny (Coleoptera). *Carabid Beetles: Their Evolution, Natural History, and*

Classification (ed. by T.L. Erwin, G.E. Ball and D.R. Whitehead), pp. 113–180. W. Junk, The Hague.

Hansen, M. (1997) Evolutionary trends in "staphyliniform" beetles (Coleoptera). *Steenstrupia*, **23**, 43–86.

Herman, L.H. (2013) Revision of the new world species of *Oedichirus* (Coleoptera: Staphylinidae: Paederinae: Pinophilini: Procirrina). *Bulletin of the American Museum of Natural History*, **375**, 1–137.

Hillis, D.M. & Dixon, M.T. (1991) Ribosomal DNA: molecular evolution and phylogenetic inference. *Quarterly Review of Biology*, **66**, 411–453.

Hlaváč, P. & Chandler, D.S. (2005) World catalog of the species of Tyrini with a key to genera (Coleoptera: Staphylinidae: Pselaphinae). *Folia Heyrovskyana*, **13**, 81–143.

Hunt, T., Bergsten, J., Levkanicova, Z. *et al.* (2007) A comprehensive phylogeny of beetles reveals the evolutionary origins of a superradiation. *Science*, **318**, 1913–1916.

Jeannel, R. (1950a) Coléoptéres psélaphides. *Faune de France*, **53**, 1–421.

Jeannel, R. (1950b) Géonémie des psélaphides de l'Afrique intertropicale. *Memoires du Museum National d'Histoire. Serie A, Zoologie*, **2**, 1–48.

Jeannel, R. (1954) Les pselaphides de Madagascar. *Memoires de l'Institut Scientifique de Madagascar*, **4**, 139–344.

Jeannel, R. (1955) Les psélaphides de l'Afrique Australe. *Mémoires du Muséum d'Histoire Naturelle. N.S. Série A, Zoologie*, **9**, 1–196.

Jeannel, R. (1959) Révision des psélaphides de l'Afrique intertropicale. *Annales du Musée Royal du Congo Belge, Tervuren (Série 8°: Sciences Zoologiques)*, **75**, 1–742.

Jeannel, R. (1961) La Gondwanie et le peuplement de l'Afrique. *Musée Royal de l'Afrique Centrale. Annales. Série in 8°. Sciences Zoologiques*, **102**, 1–82.

Jell, P.A. (2006) The fossil insects of Australia. *Memoirs of The Queensland Museum*, **50**, 1–124.

Jell, P.A. & Duncan, P.M. (1986) Invertebrates, mainly insects, from the freshwater, lower Cretaceous, Koonwarra Fossil Bed (Korumburra Group), South Gippsland, Victoria. *Plants and Invertebrates from the Lower Cretaceous Koonwarra Fossil Bed, South Gippsland, Victoria* (ed. by P.A. Jell and J. Roberts), pp. 1–205. Memoir of the Association of Australasian Palaeontologists, Sydney, Australia.

Katoh, K. & Standley, D.M. (2013) MAFFT multiple sequence alignment software version 7: improvements in performance and usability. *Molecular Biology and Evolution*, **30**, 772–780.

Kistner, D.H. (1982) The social insects' bestiary. *Social Insects* (ed. by H.R. Hermann), pp. 1–244. Academic Press, New York, NY, U.S.A.

Kulicka, R. & Ślipiński, A. (1996) A review of the Coleoptera inclusions in the Baltic amber. *Prace Muzeum Ziemi*, **44**, 13–20.

Kurbatov, S.A. (2007) Revision of the genus *Intestinarius* gen. n. from Southeast Asia, with notes on a probable autapomorphy of Batrisitae (Coleoptera: Staphylinidae: Pselaphinae). *Russian Entomological Journal*, **16**, 275–289.

LaPolla, J.S. & Dlussky, G.M. (2013) Ants and the fossil record. *Annual Review of Entomology*, **58**, 609–630.

Lawrence, J.F. & Newton, A.F. (1982) Evolution and classification of beetles. *Annual Review of Ecology and Systematics*, **13**, 261–290.

Leschen, R.A.B. (1991) Behavioral observations on the myrmecophile *Fustiger knausii* (Coleoptera: Pselaphidae: Clavigerinae) with a discussion of grasping notches in myrmecophiles. *Entomological News*, **102**, 215–222.

Lewis, P.O. (2001) A likelihood approach to estimating phylogeny from discrete morphological character data. *Systematic Biology*, **50**, 913–925.

Löbl, I. (2000) *Pachacuti chandleri* sp. n. and *Sabarhytus kinabalu* gen. et sp. n. with comments on Arhytodini and Pselaphini (Coleoptera, Staphylinidae, Pselaphinae). *Biological Journal of the Linnean Society*, **55**, 143–149.

Löbl, I. & Kurbatov, S.A. (1995) New *Tychobythinus* (Coleoptera, Staphylinidae, Pselaphinae) from East and Southeast Asia. *Mitteilungen der Schweizerischen Entomologischen Gesellschaft*, **68**, 297–304.

Maddison, W.P. & Maddison, D.R. (2011) *Mesquite: A Modular System for Evolutionary Analysis*. Version 2.75 [WWW document]. URL mesquite.project.org [accessed on January 2014].

McKenna, D.D., Farrell, B.D., Caterino, M.S. *et al.* (2014) Phylogeny and evolution of Staphyliniformia and Scarabaeiformia: forest litter as a stepping stone for diversification of nonphytophagous beetles. *Systematic Entomology*, **40**, 35–60.

Miller, M.A., Pfeiffer, W. & Schwartz, T. (2010) Creating the CIPRES Science Gateway for inference of large phylogenetic trees. *Proceedings of the Gateway Computing Environments Workshop (GCE)*. 14 Nov 2010 (ed. by M.A. Miller, W. Pfeiffer and T. Schwartz), pp. 1–8, New Orleans, Louisiana.

Moreau, C.S. & Bell, C.D. (2013) Testing the museum versus cradle tropical biological diversity hypothesis: phylogeny, diversification, and ancestral biogeographic range evolution of the ants. *Evolution*, **67**, 2240–2257.

Nel, A., Perrault, G., Perrichot, V. & Néradeau, D. (2004) The oldest ant in the lower Cretaceous amber of Charente-Maritime (SW France) (Insecta: Hymenoptera: Formicidae). *Geologica Acta*, **2**, 23–29.

Newton, A.F. & Chandler, D.S. (1989) World catalog of the genera of Pselaphidae (Coleoptera). *Fieldiana Zoology*, **53**, 1–110.

Newton, A.F. & Thayer, M.K. (1995) Protopselaphinae new subfamily for *Protopselaphus* new genus from Malaysia, with a phylogenetic analysis and review of the Omaliine Group of Staphylinidae including Pselaphidae (Coleoptera). *Biology, Phylogeny, and Classification of Coleoptera: Papers Celebrating the 80th Birthday of Roy A. Crowson* (ed. by J. Pakaluk and A. Ślipiński), pp. 221–320. Muzeum i Instytut Zoologii PAN, Warszawa.

Nomura, S. (1991) Systematic study on the genus *Batrisoplisus* and its allied genera from Japan (Coleoptera, Pselaphidae). *Esakia*, **30**, 1–462.

Ogg, J.G., Hinnov, L.A. & Huang, C. (2012) Cretaceous. *The Geologic Time Scale* (ed. by F.M. Gradstein, J.G. Ogg, M.D. Schmitz and G.M. Ogg), pp. 793–853. Elsevier, Boston, Massachusetts.

Ohishi, H. (1986) Consideration of internal morphology for the taxonomy of Pselaphidae. *Papers on Entomology Presented to Prof. Takehiko Nakane in Commemoration of his Retirement*, pp. 1–21. Japanese Society of Coleopterology, Tokyo, Japan.

Olson, D.M. (1994) The distribution of leaf litter invertebrates along a Neotropical altitudinal gradient. *Journal of Tropical Ecology*, **10**, 129–150.

Park, O. (1932) The myrmecocoles of *Lasius umbratus mixtus aphidicola* Walsh. *Annals of the Entomological Society of America*, **25**, 77–88.

Park, O. (1933) The food and habits of *Tmesiphorus costalis* Lec. (Coleop.: Pselaphidae). *Entomological News*, **44**, 149–151.

Park, O. (1942) *A Study in Neotropical Pselaphidae*, Vol. 1. Northwestern University, Evanston, Chicago, Illinois.

Park, O. (1951) Cavernicolous pselaphid beetles of Alabama and Tennessee, with observations on the taxonomy of the family. *Geological Survey of Alabama Museum Paper*, **31**, 1–107.

Park, O. (1953) New or little known pselaphid beetles of the United States, with observations on Taxonomy and evolution of the family Pselaphidae. *Bulletin of the Chicago Academy of Sciences*, **9**, 249–283.

Park, O. (1964) Observations on the behaviour of myrmecophilous pselaphid beetles. *Pedobiologia*, **4**, 129–137.

Park, J.S. & Carlton, C.E. (2014) *Pseudostenosagola*, a new genus from New Zealand (Coleoptera: Staphylinidae: Pselaphinae: Faronitae). *Annals of the Entomological Society of America*, **107**, 734–739.

Parker, J. (2016) Myrmecophily in beetles (Coleoptera): evolutionary patterns and biological mechanisms. *Myrmecological News*, **22**, 65–108.

Parker, J. & Grimaldi, D.A. (2014) Specialized myrmecophily at the ecological dawn of modern ants. *Current Biology*, **24**, 2428–2434.

Parker, J. & Maruyama, M. (2013) *Jubogaster towai*, a new Neotropical genus and species of Trogastrini (Coleoptera: Staphylinidae: Pselaphinae) exhibiting myrmecophily and extreme body enlargement. *Zootaxa*, **3630**, 369–378.

Peris, D., Chatzimanolis, S. & Delclòs, X. (2014) Diversity of rove beetles (Coleoptera: Staphylinidae) in early Cretaceous Spanish amber. *Cretaceous Research*, **48**, 85–95.

Raffray, A. (1890a) Etude sur les pselaphides. VI. Diagnoses des espèces nouvelles sur lesquelles sont fondés des genres nouveaux. *Revue d'Entomologie*, **9**, 193–219, pls. 2–3.

Raffray, A. (1890b) Étude sur les psélaphides. *Revue d'Entomologie*, **9**, 1–28, pl. 1.

Raffray, A. (1908) Coleoptera fam. Pselaphidae. *Genera Insectorum* (ed. by P. Wytsman), pp. 1–487. V. Verteneuil & L. Desmet, Bruxelles.

Rambaut, A. (1996) *Se-Al: Sequence Alignment*.

Rambaut, A., Suchard, M.A., Xie, D. & Drummond, A.J. (2013) *Tracer Version 1.6* [WWW document]. URL http://beast.bio.ed.ac.uk/Tracer [accessed on January 2014].

Reichle, D.E. (1966) Some pselaphid beetles with boreal affinities and their distribution along the postglacial fringe. *Systematic Zoology*, **15**, 330–344.

Reichle, D.E. (1967) The temperature and humidity relations of some bog pselaphid beetles. *Ecology*, **48**, 208–215.

Ronquist, F., Teslenko, M., van der Mark, P. *et al.* (2012) MrBayes 3.2: efficient Bayesian phylogenetic inference and model choice across a large model space. *Systematic Biology*, **61**, 539–542.

Ryvkin, A.B. (1985) Beetles of the family Staphylinidae from the Jurassic of Transbaikalia. *Trudy Paleontologicheskogo Instituta, Akademia Nauk SSSR*, **211**, 88–91.

Sakchoowong, W., Nomura, S. & Chanpaisaeng, J. (2007) Comparison of extraction efficiency between Winkler and Tullgren extractors for tropical leaf litter macroarthropods. *Thai Journal of Agricultural Science*, **40**, 97–105.

Schaufuss, L.W. (1890) System-schema der Pselaphiden, ein Blick in die Vorzeit, in die Gegenwart und In die Zukunft. *Tijdschrift voor Entomologie*, **33**, 101–162.

Schomann, A., Afflerbach, K. & Betz, O. (2008) Predatory behaviour of some Central European pselaphine beetles (Coleoptera: Staphylinidae: Pselaphinae) with descriptions of relevant morphological features of their heads. *European Journal of Entomology*, **105**, 889–907.

Sereno, P.C. (2007) Logical basis for morphological characters in phylogenetics. *Cladistics*, **23**, 565–587.

Shi, G., Grimaldi, D.A., Harlow, G.E. *et al.* (2012) Age constraint on Burmese amber based on U-Pb dating of zircons. *Cretaceous Research*, **37**, 155–163.

Solodovnikov, A., Yue, Y., Tarasov, S. & Ren, D. (2013) Extinct and extant rove beetles meet in the matrix: early Cretaceous fossils shed light on the evolution of a hyperdiverse insect lineage (Coleoptera: Staphylinidae: Staphylininae). *Cladistics*, **29**, 360–403.

Thayer, M.K., Newton, A.F. & Chatzimanolis, S. (2012) *Prosolierius*, a new mid-Cretaceous genus of Solieriinae (Coleoptera: Staphylinidae) with three new species from Burmese amber. *Cretaceous Research*, **34**, 124–134.

Tikhomirova, A.L. (1968) Staphylinid beetles of the Jurassic of the Karatau (Coleoptera, Staphylinidae). *Jurassic Insects of Karatau* (ed. by B.B. Rohdendorf), pp. 139–154. Akademiya Nauk SSSR, Moscow, Idaho.

Ward, P.S. (2014) The phylogeny and evolution of ants. *Annual Review of Ecology, Evolution, and Systematics*, **45**, 23–43.

Wilson, E.O. (1990) *Success and Dominance in Ecosystems: The Case of the Social Insects*. Ecology Institute, Oldendorf/Luhe.

Wilson, E.O. & Hölldobler, B. (2005) The rise of the ants: a phylogenetic and ecological explanation. *Proceedings of the National Academy of Sciences of the United States of America*, **102**, 7411–7414.

Yamamoto, S. (2016) The first fossil of dasycerine rove beetle (Coleoptera: Staphylinidae) from upper Cretaceous Burmese amber: phylogenetic implications for the omaliine group subfamilies. *Cretaceous Research*, **58**, 63–68.

Accepted 4 January 2016
First published online 23 February 2016